EFFECT OF ELECTRICAL VEHICLES ON RESIDENTIAL DISTRIBUTION SYSTEMS

A Thesis

Submitted to the Graduate Faculty of the
Louisiana State University and
Agricultural and Mechanical College
in partial fulfillment of the
requirements for the degree of
Masters of Science in Electrical Engineering

In

The Department of Electrical and Computer Engineering

By
Paul Haley
B.S., Louisiana State University, 2010
August 2012

TABLE OF CONTENTS

LIST OF TABLES

LIST OF FIGURES

ABSTRACT

This thesis focuses on the present state of electrical vehicles (EVs) in the market and the effects that these vehicles could have on residential distribution systems. The current EVs available on the market and the current level of market penetration were investigated. Advantages and disadvantages of EVs from a consumer and governmental perspective were identified. The efficiencies of the whole energy delivery process of electrical vehicles and gasoline vehicles were estimated. Efficiency estimation was used to estimate the impact of EVs on the consumption of fossil fuels and emission of greenhouse gases.

Measurement of an EV battery charging cycle and modeling of a residential power system with EV battery charger loads was performed. A computer model was programmed in Matlab to perform harmonic analysis using data from a real residential system. Using this computer model a worst case study was performed, and the level of EV penetration in the system required to cause excessive harmonic distortion was obtained.

CHAPTER 1. INTRODUCTION

1.1 Electrical Vehicles Background

The development of electrical vehicles (EVs) started in the second half of the 19th century, and they were used in Europe starting in the early 1880s. Electrical vehicles started gaining popularity in the United States automobile market in the 1900s which until that time had been dominated by steam powered vehicles [1]. Around the same time U.S. auto manufacturers such as Oldsmobile and Ford started mass production of affordable gasoline vehicles adding further competition in the market. In the 1920s roads and infrastructure were significantly developed providing the ability to drive great distances. Gasoline vehicles in that time, like the popular Ford Model T, could drive at speeds over 40 mph and distances over 200 miles on a full tank of gasoline [2] [3] [4]. Electrical cars could only reach speeds up to 20 mph and distances of 40 miles on a fully charged battery. Consequently, EVs were not able to compete, and gasoline vehicles continued to gain popularity. Today more than 99% of passenger vehicles have gasoline engines.

However, driven by concerns about greenhouse gas emissions and depletion of non-renewable energy sources EVs have once again entered the market. Technological advancements in electrical motors, solid state electronics, batteries, and computers for use in EV systems have drastically improved the range, speed, and torque of EVs. Proponents of electrical cars claim that they are "quieter, cleaner, and cheaper to run than gasoline-powered cars" [5]. Despite these claims, automobile manufacturers in the U.S. have released few models of electrical vehicles in the past two decades, and those that have been released so far have had extremely poor sales compared to their gasoline engine counterparts. In 2011 around 17,000 EVs and plug-in hybrids were sold in the U.S. out of about 13 million passenger cars total [6] [7].

The U.S. government is particularly interested in reducing carbon emissions and dependence on oil. Because of this, government at the state and federal level has passed legislation designed to influence the passenger vehicles market. The American Recovery and Reinvestment Act of 2009 created a federal tax credit of around $7,500 for most plug-in Electrical passenger vehicles purchased after 2009 [8]. The California Air Resources Board famously passed a mandate in 1996 requiring that 5% of new vehicles for sale in California would have to be zero-emissions vehicles by 1998 [9]. This mandate has been updated and revised several times to continuously place low emissions standards on the automotive industry, and there is much debate among corporations, environmentalist groups, and government representatives about how much involvement the government should have in the development of Electrical vehicles [10]. More information on the various forces on electrical vehicles in the market will be discussed in chapter 2.

1.2 Challenges for Power Distribution

A major issue with the growing interest in electrical vehicles is preparing the power system to accommodate these EV battery charger loads. Possible problems include exceeding ratings of distribution equipment and home electrical systems, reduction of voltage profile, low power factor, and harmonic distortion. The extent of each of these problems depends on the load characteristics of the battery chargers and the power system.

EV battery chargers require active power in the range of 2 to 4 kW. This is comparable to the power of a large central air conditioner in a home, but an electrical vehicle would require this power for up to 10 hours of uninterrupted charging on a 240 V home charging station. There is concern that if there are many of these chargers in a distribution system transformers could be

overloaded. Additionally, the high current required by such a load could cause noticeable voltage drops in the distribution system, reducing the voltage profile. The simplest solution to both of these problems is to upgrade distribution system components.

Another issue is generation of current harmonics by battery chargers. This might increase the level of harmonic distortion in the distribution system and cause some detrimental effects on the power system equipment and supplied loads. In particular, harmonics can degrade the effectiveness of capacitive compensators installed in the distribution system to improve the power factor. This could be a matter of concern for distribution systems engineers, who are required to keep the level of harmonic distortion within the limits set in IEEE Std. 519.

Because of all these power system challenges, it is important for power utilities to know the characteristics of EV charger loads. This knowledge will help them to prepare for increasing numbers of these loads in the power system. Many of the upgrades to the system could require detailed planning and long construction times, so it is also important to have an idea of how soon electrical vehicles could reach significant market penetration. While it is impossible to accurately predict how long this could take, a general idea can be obtained by examining the forces in the market that affect EV dissemination.

1.3 Objectives

The objective of this thesis is to present the current state of the electrical vehicles market and to predict the impact of such vehicles upon residential distribution systems. In particular, forces that affect dissemination of EVs will be identified and examined, and current market penetration will be discussed. Major forces on demand include convenience and cost of EVs compared to their competitors, specifically gasoline and hybrid vehicles. Recent government

influence will also be discussed. The reasons for government involvement will be investigated, and the environmental impact of EVs will be estimated.

Moreover, this thesis will investigate what the load characteristics of EV battery chargers are and what problems these loads could realistically cause in residential power systems. The problems that will be examined include exceeding equipment ratings, low voltage profile, low power factor, and harmonic distortion.

1.4 Approach to Objectives

Some parts of this research will be a compilation of information from news articles and other research papers, but also some valuable information will be obtained from first-hand measurements and computer modeling.

First the different electrical drive technologies will be differentiated, and the conveniences and inconveniences of EV technology will be discussed. The cost of vehicles to consumers will be compared using a basic amortization time calculation for an EV and a comparable GV by the same manufacturer. To determine recent EV market penetration and sales performance, information will be presented from government documents, news articles, and studies published in scientific journals. To explore government influence on the market, recent legislation will be discussed, and the efficiency and environmental impact of EVs will be compared to GVs. Each component of the systems that provide energy to the EV and GV will be analyzed. The efficiencies of each component will be estimated by using the most credible data available from various manufacturers and published studies. In some cases data from secondhand or third hand sources will be used because of lack of data from more reliable sources.

Load characteristics of EVs will be obtained from recognized standards and published studies and by taking current and voltage measurements of an EV charging cycle. This data will be used to model a residential distribution system with EV battery charger loads. The model will be programmed in Matlab to evaluate the RMS voltages of the system as well as the voltage CRMS harmonic values and total harmonic distortion.

CHAPTER 2. ELECTRICAL VEHICLES IN THE U.S. MARKET

2.1 Types of Electrical Drives

2.1.1 Hybrid Vehicles

There are three different structures used to drive cars with electrical motors. These structures are commonly known as hybrid, plug-in hybrid (PHEV), and electrical vehicles (EV). While hybrids will not be charged from the distribution grid, they are important in determining the success of EVs and PHEVs in the market.

Hybrids require a combustion engine to run, but the use of an electrical drive system in combination with the combustion engine makes hybrids more fuel efficient than traditional GVs. There are several hybrid configurations of which a parallel type is the most popular. In this configuration the shaft of an induction or synchronous machine is coupled to the shaft of the combustion engine through a differential. Hybrids can also have a series configuration where the gasoline engine is coupled to a generator charging a battery which supplies energy to the electrical drive system. In all configurations there is no need for a mechanical gear transmission box, since the speed and torque of an electrical motor can be smoothly adjusted by changing frequency and current RMS. The main advantage that the electrical drive system provides is the bidirectional flow of energy. While the car is braking, the electrical machine operates in generator mode, and much of the vehicle's kinetic energy is converted to electric energy which is stored in the battery. Since combustion engines do not have this ability, the kinetic energy of the car is simply lost in brakes as heat from friction. Because of this hybrids are more efficient than traditional combustion engine powered vehicles. Specifications of the 2011 models of some of the most common hybrids in the U.S. are listed in Table 2.1 on the following page.

Table 2.1 Common U.S. hybrid cars specifications

Car model	Gas Eng volume	Gas Eng power	Elec Mot power	Battery storage	mpg (city)	Price
Honda Civic Hybrid	1.5 l	110hp	23 hp	0.6 kWh	44 mpg	$24 050
Honda CR-Z Hybrid	1.5 l	122 hp	13 hp	0.6 kWh	31 mpg	$19 345
Toyota Prius	1.8 l	98 hp	38 hp	1.8 kWh	50 mpg	$23 520
Lexus HS Hybrid	2.4 l	187 hp	N/A	N/A	35 mpg	$36 300
Ford Escape Hybrid	2.5 l	177 hp	24 hp	0.6 kWh	34 mpg	$30 825
Toyota Highlander Hybrid	3.5	280 hp	61 hp	N/A	28 mpg	$37 490

2.1.2 Plug-in Hybrid Electrical Vehicles

Plug-in hybrid electrical vehicles (PHEVs) or plug-in hybrids have a gasoline engine and electrical motor configuration like a normal hybrid, but they have been designed with a larger battery that can be charged from the electrical power distribution system. Lithium-ion batteries are typically used for this purpose. Most PHEVs are designed so that the owner can do most normal city driving using only battery power, and the combustion engine is only used when driving long distances. Specifications of some 2011 plug-in hybrids are listed in Table 2.2 below.

Table 2.2 U.S. plug-in hybrids specifications

Car model:	Gas Eng volume	Gas Eng power	Elec Mot power	Battery storage	Elec Mot range	Price
Chevrolet VOLT	1.4 l	83 hp	111 kW	16 kWh	35 mi	$39 145
Toyota Prius ZVW30	1.8 l	98 hp	60 kW	1.3 kWh	14.3 mi	$32 760
Fisker Karma	2.0 l	0	300 kW	22 kWh	32 mi	$95 900
Suzuki Swift PHEV*	0.66 l	NA	55 kW	2.7 kWh	19 mi	$24 882
Ford C_Max Energi*	NA	NA	NA	9 kWh	20 mi	$35 000
Volvo V70*	NA	NA	NA	11 kWh	30 mi	NA
Volvo V60 Diesel*	2.4 l	215 hp	53 kW	12 kWh	30 mi	$50 000

2.1.3 Electrical Vehicles

Electrical vehicles (EVs) do not have combustion engines. They are driven only using energy stored in batteries which are charged from the power distribution system. EVs require large electric energy storage capacity, and typically lithium-ion type batteries are used for this. Specifications of the most popular 2011 model EVs are listed in Table 2.3.

Table 2.3 U.S. electrical vehicles specifications

Nissan LEAF ($35,200)	
Motor	80 kW AC synchronous
Battery	24 kWh lithium-ion
Charger	3.3 kW on-board
Supply voltage	120 V, 240 V
Range	100 miles/charge. (EPA: 73 miles/charge).
Velocity	90 mph
Charging time	20 hours at 120 V, 7 hours at 240 V [12]
Charging current	27.5 A
Mitsubishi MiEV ($29,125)	
Motor	47 kW permanent magnet synchronous
Battery	16 kWh lithium-ion
Charger	1.6 kW at 120 V 3.6 kW at 240 V
Supply voltage	120 V, 240 V
Range	80 miles (EPA: 63 miles/charge)
Velocity	81 mph
Charging time	22 hours at 120 V, 7 hours at 240 V [11]
Charging current	18 A at 120V
Ford/Azure Dynamics Transit Connect Electric ($60 000)	
Motor	60 kW 3-ph induction
Battery	28 kWh lithium-ion
Charger	3.3 kW
Supply voltage	120 V, 240 V
Range	80 miles (EPA: 56 miles/charge)
Velocity	75 mph
Charging time	15 hours at 120 V, 8 hours at 240 V
Charging current	30 A at 120 V; 15A at 240V

Table 2.3 continued

Tesla Roadster ($98 000)	
Motor	215 kW induction motor with variable freq.
Battery	28 kWh lithium-ion
Charger	16.8 kW
Supply voltage	120 V, 240 V
Range	244 miles/charge
Velocity	125 mph
Charging time	3.5 hours at 240 V
Charging current	70 A at 240 V

2.2 Advantages and Disadvantages of EVs for Consumers

2.2.1 Convenience of EVs

EVs are in some ways more convenient to use than GVs. EVs are designed so that the driving range on a full battery is comparable to the average daily driving distance, equal approximately 33 miles. Drivers would use their cars to drive around town and commute to work, and at the end of the day they would return home and plug the car into the charging station to charge overnight. In addition to never having to visit a gas station, EV drivers will never have to get an oil change. So for drivers who like the idea of a low maintenance car, EVs have some advantages.

Unfortunately the disadvantages of EVs are significant. While the range of most recent EVs is enough for driving in town, using an EV to travel out of town is not reasonable. Without easily accessible distributed charging infrastructure, drivers will have to return home to recharge. Thus, drivers are limited to a travel distance of half of the total driving mileage of the fully charged EV. Figure 2.1 shows a visual comparison of the practical driving distance from home of the most popular EVs and PHEVs in the U.S.

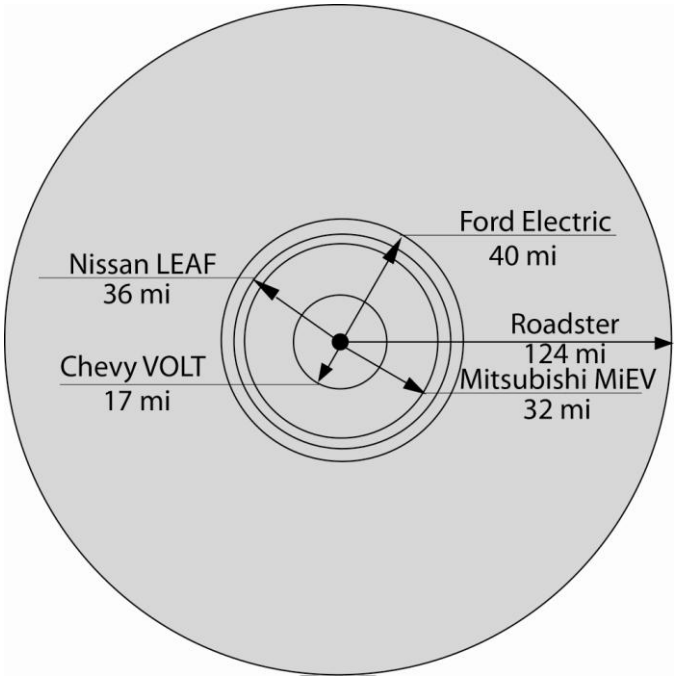

Figure 2.1 Practical travel distance from home of EVs in the U.S.

Many changes to infrastructure have been proposed to allow EV owners to drive farther, but unfortunately all of them have significant problems. There are some 240 V charging stations which are accessible to the public. Unfortunately there aren't many in most parts of the U.S., and, just like home EV battery chargers, they take around eight hours to fully charge a depleted battery. 400 V fast charging stations are also being developed, but they are only in the testing stage and not ready for implementation in the power grid. Even if these fast chargers were available, they would still be inconvenient compared to filling up a gas tank since they take 30 minutes to charge a battery to 80% capacity. The charging current of lithium-ion batteries is strongly limited, so the charging time cannot be substantially reduced. Automated battery swapping stations are also being developed by Better Place, an EV development company based in Palo Alto, CA [11]. These stations look like car washes and could swap a depleted battery for a fully charged one in less than one minute. Unfortunately these too are still in the testing phase,

and many automobile manufacturers are unsupportive because of concerns about lack of standardized batteries and possible damage caused by frequent replacement. According to [12], in 2011, the average cost of lithium-ion batteries was $800 per kWh. Considering that most EVs on the market have battery capacity in the range of 16~28 kWh, batteries for EVs cost $13,000~$22,000 making the possibility of damage from replacement significant.

Because of this range limitation an entirely electrical car might be regarded only as a secondary car. For people who cannot afford a second car, a plug-in hybrid could be a better option. A potential new buyer who desires a "green car" without range restrictions can choose between a hybrid and a plug-in hybrid.

2.2.2 Cost Comparison of PHEVs and GVs

Plug-in hybrid cars are typically designed with a driving range on battery power comparable with the average daily driving distance of 33 miles. This means that most PHEV drivers will mainly use the energy stored in the battery to drive, using the gasoline engine only in situations when the driving distance exceeds the battery range. Because of this PHEVs are sometimes referred to as extended-range electrical vehicles. PHEVs would have essentially the same environmental benefits that standard EVs have without the range limitations. This means that from a national perspective PHEVs are advantageous, but often consumers are more concerned with the price of the car than the national benefits.

At present prices of gas and electric energy, cost of driving a plug-in hybrid car is lower than a comparable gasoline-driven car. Gasoline cars cost less to buy than plug-in hybrids, however. Thus, the decision on selecting between a plug-in hybrid and common hybrid or GV can be based on evaluation of the amortization time.

Assume that the price of a plug-in hybrid is P_E while the price of another car, equivalent with respect to performance and driving comfort is P_G. Thus the price difference in $ is $\Delta P = P_E - P_G$. If the average annual driving distance is D = 15,000 miles/year, then driving a plug-in hybrid with the driving efficiency d_E in [miles/kWh] at electric energy price of p_E in [$/kWh], cost per year

$$C_E = \frac{D}{d_E} \times p_E .$$

Driving a gasoline car with the driving efficiency d_G in [miles/gal] or mpg, at gas price of p_G in [$/gal], cost per year

$$C_G = \frac{D}{d_G} \times p_G .$$

Amortization of the higher price of the plug-in hybrid, by lower driving cost, in years of driving is

$$A = \frac{P_E - P_G}{C_G - C_E}.$$

For Chevrolet VOLT, ($39,145) which has driving efficiency d_E= 35 miles/16 kWh = 2.2 miles/kWh, at electrical energy price of p_E = 0.11 $/kWh, the annual cost of energy is

$$C_E = \frac{D}{d_E} \times p_E = \frac{15000\,[\frac{\text{miles}}{\text{year}}]}{2.2\,[\frac{\text{miles}}{\text{kWh}}]} \times 0.11\,[\frac{\$}{\text{kWh}}] = 750\,[\frac{\$}{\text{year}}].$$

The closest gasoline model from the same company seems to be Chevrolet Cruze, ($16,525) with city mpg of 22 miles/gallon. At gasoline price of p_G = 3.2 $/gal., the annual cost of fuel is

$$C_{\mathrm{G}} = \frac{D}{d_{\mathrm{G}}} \times p_{\mathrm{G}} = \frac{15000\,[\frac{\mathrm{miles}}{\mathrm{year}}]}{22\,[\frac{\mathrm{miles}}{\mathrm{gal}}]} \times 3.2\,[\frac{\$}{\mathrm{gal}}] = 2182\,[\frac{\$}{\mathrm{year}}].$$

Thus, amortization time is

$$A = \frac{P_{\mathrm{E}} - P_{\mathrm{G}}}{C_{\mathrm{G}} - C_{\mathrm{E}}} = \frac{39145 - 16525}{2182 - 750} = 15.6 \text{ years}.$$

Such a long amortization time might be difficult to accept for a potential buyer. Even with the government incentive of $7,500, amortization time would be

$$A = \frac{P_{\mathrm{E}} - P_{\mathrm{G}} - \$\,Inc.}{C_{\mathrm{G}} - C_{\mathrm{E}}} = \frac{39145 - 16525 - 7500}{2182 - 750} = 10.5 \text{ years}.$$

This long amortization time explains why of 10 000 Chevrolet VOLTSs built in 2011, only 3,700 were sold. It should be noted that state incentives for EVs vary, and including the state tax incentives the amortization time could be reduced by another year or two.

EVs and plug-in hybrids compete now with common hybrid car with very high fuel efficiency. For example, similar to Chevrolet VOLT, Honda Civic Hybrid ($24,500) has fuel efficiency in city of d_{GHb}= 44 miles/gallon. The annual cost of Honda fuel, C_{GH}, is

$$C_{\mathrm{GH}} = \frac{D}{d_{\mathrm{GH}}} \times p_{\mathrm{G}} = \frac{15000\,[\frac{\mathrm{miles}}{\mathrm{year}}]}{44\,[\frac{\mathrm{miles}}{\mathrm{gal}}]} \times 3.2\,[\frac{\$}{\mathrm{gal}}] = 1091\,[\frac{\$}{\mathrm{year}}].$$

With respect to Chevrolet Cruze ($16,525, 22 mpg), amortization time of Honda Civic Hybrid is

$$A = \frac{24500 - 16525}{2182 - 1091} = 7.3 \text{ years}.$$

For Toyota Prius hybrid, 2010, ($23,520) with the fuel efficiency d_{GT}=50miles/gallon, the annual cost of fuel is

$$C_{\mathrm{GT}} = \frac{D}{d_{\mathrm{GT}}} \times p_{\mathrm{G}} = \frac{15000\,[\frac{\mathrm{miles}}{\mathrm{year}}]}{50\,[\frac{\mathrm{miles}}{\mathrm{gal}}]} \times 3.2\,[\frac{\$}{\mathrm{gal}}] = 960\,[\frac{\$}{\mathrm{year}}].$$

and the amortization time with respect to Chevrolet Cruze is

$$A = \frac{23520 - 16525}{2182 - 960} = 5.7 \text{ years.}$$

Thus, common hybrids which do not require charging batteries from the power grid are main competitors to plug-in hybrids. The number of such hybrids is increasing. Almost every main car manufacturer has one or even a few hybrids in production or plans. This means that currently common hybrids prevail in the competition with the plug-in hybrids or entirely EVs. A major reduction in the cost of plug-in hybrids is needed to change the present situation. Without it, it is unlikely that such cars will occur in a considerable number on the car market. Cost of the lithium-ion battery is the main cost component of plug-in hybrids. According [12] the average cost of lithium-ion batteries in 2011 was $800 per kWh. For example, in the case of the 2011 Chevrolet Volt, with a 16 kWh battery, this cost is 16 x $800 = $12,800 which is more than half of the price difference between the Chevrolet Volt and the closest equivalent to the Volt, the Chevrolet Cruze, equal to $22,620.

2.2.3 Consumer Perception of "Green Cars"

For some consumers cost is not a significant factor in choosing a car. The perception that they are helping to protect the environment or that they are on the cutting edge of technology may be enough to convince them to buy an EV. Indeed this perception that EVs are "clean" or "green" is emphasized in advertisements such as the Nissan LEAF slogan, "100% electric. Zero gas. Zero tailpipe [13]." The EPA ratings which are displayed on the windows of new cars also

claim that EVs have zero greenhouse gas tailpipe emissions. This advertisement is misleading since most electrical energy generation causes greenhouse gas emissions. Whether the emissions come from the tailpipe of a car or from a power generation facility is irrelevant. Still, popular opinion among consumers is that EVs are environmentally friendly. Instead of cost or convenience, this concern for the environment appears to be the main motivation for many recent EV buyers.

2.3 Current EV Market Trends and Government Influence

2.3.1 Current Market Penetration

According to some reports [14] the number of plug-in hybrids and EVs on the US market from US automobile and other manufacturers by 2011 is about 56,000 which is 0.002% of all cars in the US. Even if data on number of EVs and GVs are very inaccurate, it is clear that EVs do not penetrate the market and residential grids noticeably now. Furthermore, many of these EVs are sold to industrial and commercial companies, and consequently, such EVs are often not charged from residential distribution grids.

Major EV manufacturers have struggled to meet their sales goals. Chevy projected that in 2011 they would sell 10,000 of their PHEVs, the Volt. At the end of 2011 they only sold about 7,600. In 2012 Chevy initially estimated that they would sell 35,000 Volts, but through February they only sold about 1,600. In March of 2012 Chevy stopped production of the Volt for five weeks due to low sales [15]. The Nissan LEAF has also failed to meet sales expectations. At the start of 2011 Nissan predicted that 20,000 LEAFs would be sold in the U.S. that year. By May Nissan changed its estimate to between 10,000 and 12,000. At the end of 2011 about 9,700 were sold [16].

2.3.2 Recent Market Influence

These low sales numbers are concerning for U.S. government environmental groups. Many laws creating incentives for EV and PHEV buyers have been created to encourage consumers to buy EVs and PHEVs. President Obama has been a strong supporter of "green technology" including EVs. Aside from signing the bill which created a tax credit of $7,500 for EV and PHEV buyers, he has been a major force behind funding American "Green Technology" companies. In the American Recovery and Reinvestment Act of 2009, over $12 billion was allocated for the DOE to spend on energy efficiency and on the development of energy generation using renewable resources. This allowed funding for U.S. "green technology" companies such as lithium-ion battery manufacturer A123 which received a $249 million grant from the DOE. A123 has had many problems with the quality of their products resulting in significant monetary losses and layoffs. Fisker, a recent electrical sports car manufacturer stopped ordering from A123 after receiving defective batteries which caused one of their cars to break down during a Consumer Reports test. In April 2012 an A123 battery leaked chemical vapors into a General Motors testing lab causing an explosion, and that same month the value of A123 shares had dropped by 40% since the start of the year [17].

US state governments have passed their own laws to promote EVs. Many states provide grants for electrical vehicle research, funding for EV charging infrastructure, and loans or tax credits for "green technology" related businesses. Additionally, more than half of the states in the U.S. and the District of Columbia have passed legislature providing some kind of incentives to EV buyers. Many of these incentives are rebates, tax credits, or tax exemptions which can significantly reduce the overall cost of the car. Since these incentives vary from state to state, the total EV cost to consumers will vary depending on where the car is registered. For example, EV

buyers in Colorado are eligible for a tax credit of up to $6,000 per EV purchased plus a sales tax exemption. These state incentives plus the federal $7,500 tax credit could reduce the overall cost of an EV by more than $13,500. Other incentives include access to High Occupancy Vehicle (HOV) lanes, waived parking fees, discounted toll fees, and emissions testing exemptions. The statewide government incentives for consumers who purchase EVs are shown in Table 2.4 below [18].

Table 2.4 State government incentives for EV buyers

State/Province	Tax Credits, Tax Exemptions, and Rebates	Other Incentives
Arizona	-Electric Vehicle Charging Equipment Tax Credit: $75 - Alternative Fuel Vehicle License Tax: license tax reduced -Alternative Fuel Vehicle Tax Exemption: exempt from use tax	-HOV Lane Exemption -Access to carpool parking areas
California	-Plug-In Hybrid and Zero Emission Light-Duty Vehicle Rebates: Up to $2,500 for each vehicle purchased -Additional incentive up to $3,000 for EV or PHEV in San Joaquin Valley	-HOV Lane Exemption
Colorado	-Alternative Fuel, Advanced Vehicle, and Idle Reduction Equipment Tax Credit: up to $6,000 for new EV purchased -Low Emission Vehicle Sales Tax Exemption	-HOV Lane Exemption
District of Columbia	-Reduced Registration Fee for Fuel-Efficient Vehicles - Alternative Fuel and Fuel-Efficient Vehicle Title Excise Tax Exemption	
Florida		-HOV Lane Exemption
Georgia	-Alternative Fuel Vehicle Tax Credit: 10% of cost of new EV purchased up to $2,500. -Zero Emission Vehicle Tax Credit: 20% of the cost of new EV purchased up to $5,000.	-HOV Lane Exemption
Hawaii	- Plug-In Electric Vehicle and Electric Vehicle Supply Equipment Rebates: 20% of EV cost up to $4,500, 30% of charger cost and installation up to $500	-HOV Lane Exemption
Illinois	- Alternative Fuel Vehicle and Alternative Fuel Rebates: 80% of incremental cost of EV up to $4,000 - Electric Vehicle Registration Fee Reduction	-HOV Lane Exemption
Kansas	-Alternative Fuel Vehicle Tax Credit: 40% of incremental cost of EV up to $2,400 for cars under 10,000 lbs. or 5% of cost of EV up to $750.	

Table 2.4 continued

Louisiana	-Alternative Fuel Vehicle and Fueling Infrastructure Tax Credit: Tax credit of 50% of incremental cost of purchasing EV and charger or 10% of the purchase cost up to $3,000.	
Maryland	-Plug-In Electric Vehicle Tax Credit: up to $2,000 of the imposed excise tax for EV or PHEV -Electric Truck Purchase Vouchers: $20,000 voucher for purchase of an all-electric truck over 10,000 lbs. -Electric Vehicle Supply Equipment Tax Credit: 20% of charger cost up to $400.	-HOV Lane Exemption
Michigan	-Alternative Fuel Vehicle Tax Exemption: EVs are exempt from personal property taxes.	-Alternative Fuel Vehicle Emissions Inspection Exemption
Missouri		-Alternative Fuel Vehicle Emission Inspection Exemption
Nevada		-Alternative Fuel Vehicle Parking Fee Exemption -Alternative Fuel Vehicle and Hybrid Electric Vehicle Emissions Inspection Exemption
New Jersey	- Zero Emissions Vehicle Tax Exemption: exempt from sales and use tax.	-HOV Lane Exemption -Clean Vehicle Toll Incentive: 10% off of toll fees during off-peak hours
New York		-HOV Lane Exemption
North Carolina		-HOV Lane Exemption -Plug-In Electric Vehicle Emissions Inspection Exemption
Oklahoma	-Alternative Fuel Vehicle Tax Credit: 50% of the incremental cost of EV.	
Oregon	-Alternative Fuel Vehicle and Fueling Infrastructure Tax Credit for Residents: 25% of the incremental cost of EV up to $750	
Tennessee	-Electric Vehicle Rebate: $2,500 rebate for the first 1,000 EVs sold in Tennessee, received at the time of purchase	-HOV Lane Exemption
Texas	- Clean Vehicle Replacement Vouchers: up to $3,500 in participating counties	
Utah	- Alternative Fuel and Fuel Efficient Vehicle Tax Credit: up to $605 income tax credit	-HOV Lane Exemption
Virginia		-HOV Lane Exemption -Alternative Fuel and Hybrid Electric Vehicle Emissions Testing Exemption
Washington	-Alternative Fuel Vehicle Tax Exemption: EVs exempt from state motor vehicle sales and use taxes	-Alternative Fuel and Hybrid Electric Vehicle Emissions Testing Exemption
West Virginia	- Alternative Fuel Vehicle Tax Credit: 35% of purchase price up to $7,500 for EVs under 26,000 lbs.	

Some companies are also providing their own incentives. EV charger manufacturers ECOtality and Coulomb Technologies are offering free home charging stations to new EV buyers in many large metropolitan areas. Some power utilities are offering rebates for consumers who purchase an EV and install a home EV charging station. Many utilities also provide discounted energy rates for EV owners.

2.3.3 EVs Effect on Dependence on Foreign and Non-Renewable Resources

Some of the major reasons for transitioning to EVs are to reduce dependence on foreign oil and depletion of non-renewable resources. While EVs will likely reduce dependence on oil, they may not reduce dependence on foreign resources in general. The major components that make EVs go are batteries and electrical motors, and these components require rare earth minerals which are mostly produced in China. In fact China controls over 95% of rare earth minerals including lithium used in EV batteries and ferromagnetic materials used in electrical machines for EVs [19]. Furthermore, these materials are non-renewable, and the extraction of them is difficult and can have detrimental environmental effects. According to [20], the mining and separation process leaves byproducts of acid and radioactive material which is one of the reasons that the only rare earth minerals mine in the U.S. closed in 2002. China's monopoly on these materials is a crucial factor in the EV market. While many expect lithium-ion battery prices to decrease in the future, it is also possible that this monopoly combined with the growing demand for lithium could prevent the cost of batteries from decreasing.

CHAPTER 3. ENERGY EFFICIENCY AND ENVIRONMENTAL IMPACT OF EVS

3.1 Possible Environmental Benefits

Electrical vehicles technology has been developed largely because of the idea that they could reduce dependence on nonrenewable resources and also reduce greenhouse gas emissions. In government legislation these vehicles are referred to as zero emissions vehicles (ZEVs). While the mechanism of the vehicle itself does not produce emissions, it is erroneous to conclude that using electrical vehicles does not contribute to emissions. EVs require electric energy which is produced by generation facilities. According to data from the U.S. Energy Information Administration, in 2010 69.8% of the electric energy generated in the U.S. was from burning fossil fuels [21]. This means that currently EVs still cause some greenhouse gas emissions as well as contribute to the depletion of nonrenewable energy sources. The amount of energy generated using each type of fuel is shown in a pie chart in Figure 3.1 below.

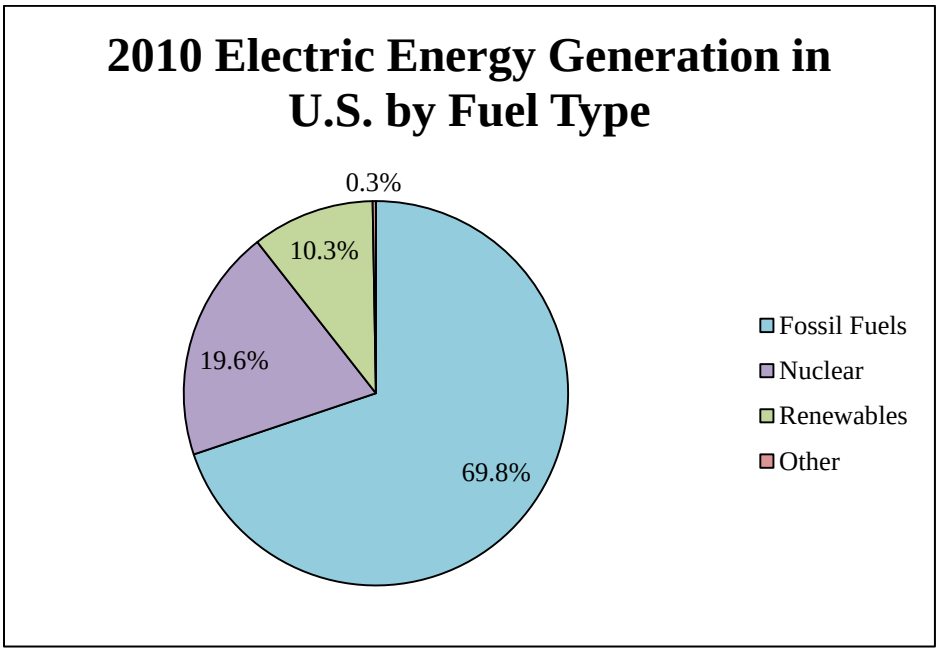

Figure 3.1 Electric energy generation in U.S. by fuel type

The essential question that must be answered is this: Do EVs demand less energy from fossil fuels than GVs? Answering this question requires analysis of the efficiency of the systems that supply energy to EVs and GVs.

3.2 Comparison of Energy Demand by GVs and EVs

3.2.1 Overview of GV and EV Energy Flow

To make a comparison of energy demand by GVs and EVs as simple as possible, at the cost of accuracy, however, it was assumed that GVs and EVs have identical mechanical parameters, meaning, they need the same amount of energy *W* for driving, and the same gasoline is used for driving a GV and for a boiler for a steam turbine in a power plant which provides electric energy for the EV.

The simplified diagrams of energy flow for a GV and EV are shown in Fig. 3.2.

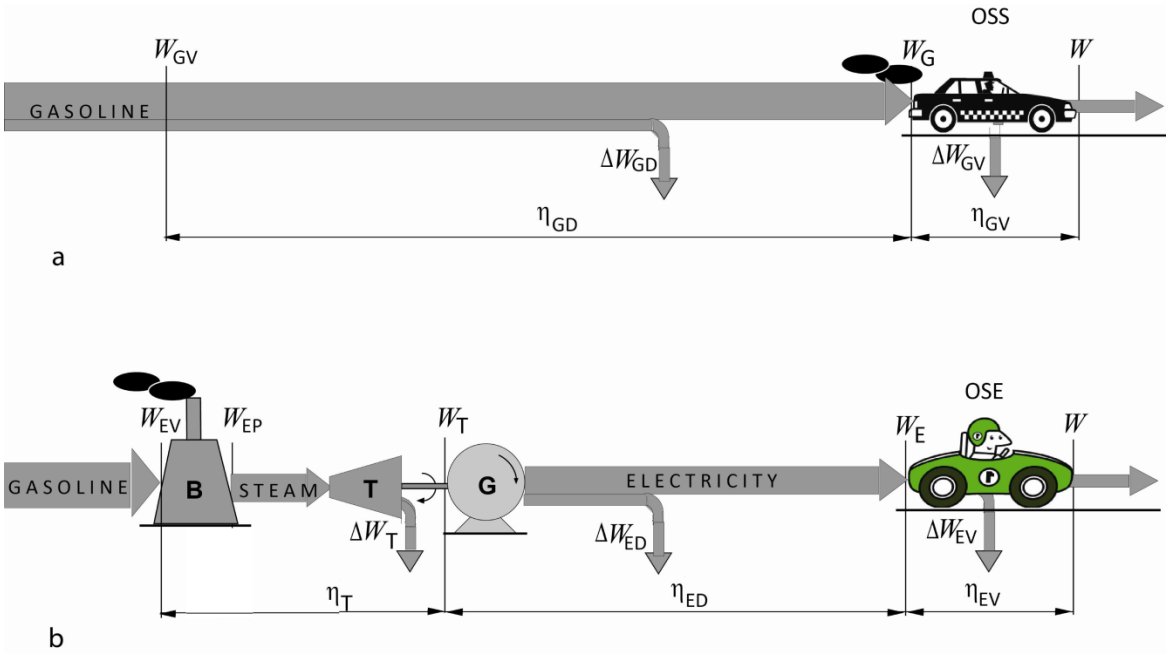

Figure 3.2 Diagrams of energy flow to GV (a) and to EV (b).

Let the energy delivered in gasoline to the car be W_G, and η_{GV} is efficiency of a GV,

$$\eta_{GV} = \frac{W}{W_G} .$$

Distribution of gasoline from refineries to gas stations involves some loss of energy ΔW_{GD}, thus this distribution operates with efficiency

$$\eta_{GD} = \frac{W_G}{W_{GV}} .$$

Energy in gasoline produced in a refinery for a single GV is

$$W_{GV} = \frac{W}{\eta_{GV} \times \eta_{GD}} .$$

Let the energy delivered by electricity to the EV be W_E while η_{EV} is electrical car efficiency,

$$\eta_{EV} = \frac{W}{W_E} .$$

Let the electric energy be produced in the generator G from energy W_T on the steam turbine shaft and next it is delivered to the EV by a transmission and distribution system with efficiency

$$\eta_{ED} = \frac{W_E}{W_T}$$

Let energy contained in gasoline used for a boiler and steam turbine system be converted into mechanical energy W_T on a steam turbine shaft with efficiency

$$\eta_T = \frac{W_T}{W_{EV}} .$$

thus, the energy in gasoline W_{EV} needed for driving a single EV is

$$W_{EV} = \frac{W}{\eta_T \times \eta_{ED} \times \eta_{EV}} .$$

Let us compare energy needed for driving otherwise identical electricity- and gasoline-driven cars:

$$\frac{W_{EV}}{W_{GV}} = \frac{\eta_{GV} \times \eta_{GD}}{\eta_T \times \eta_{ED} \times \eta_{EV}}.$$

This ratio can be rearranged to a form that emphasizes a difference in efficiencies of heat-to-mechanical energy conversion which takes place both in a combustion engine of gasoline driven car and a steam turbine, and a difference in efficiencies of gasoline and electric energy distribution.

$$\frac{W_{EV}}{W_{GV}} = \left(\frac{\eta_{GV}}{\eta_T}\right) \times \left(\frac{\eta_{GD}}{\eta_{ED}}\right) \times \frac{1}{\eta_{EV}}. \quad (1)$$

The energy demand of an EV versus a mechanically equivalent GV, meaning the ratio W_{EV}/W_{GV} depends on the ratio of efficiencies of conversion of the heat energy to mechanical energy (η_{GV}/η_T), which takes place both in a steam turbine and in a combustion engine of gasoline-driven cars, on the ratio of efficiencies of gasoline and electricity distribution (η_{GD}/η_{ED}) and on the electrical car efficiency, η_{EV}.

3.2.2 Efficiency of Heat to Mechanical Energy Conversion

Efficiency of the heat to mechanical energy conversion, both in a steam turbine and in combustion engines is confined by efficiency of the Carnot process, which is determined by temperatures of heat reservoirs on both sides of the heat-driven engine. If T_H is temperature, in Kelvin degrees, of a hot temperature reservoir and T_C is temperature of a cool temperature reservoir, then efficiency of the engine cannot be higher than

$$\eta_{HC} = 1 - \frac{T_C}{T_H}.$$

According to [22], the maximum temperature of hot steam is T_H = 543 [^{0}C] = 811[^{0}K] and it can be cooled to T_C = 43 [^{0}C] = 316 [^{0}K], which gives the upper limit of the steam turbine efficiency

$$\eta_{HC} = 1 - \frac{T_C}{T_H} = 1 - \frac{316}{811} = 0.61.$$

Due to friction and internal losses of energy, steam turbine generators do not have this efficiency, but according to [23], operate with efficiency up to approximately η_T = 0.37.

This value is much lower than the upper limit of the conversion efficiency, despite the fact that the turbine construction and operation is optimized to have the highest efficiency possible.

The efficiency of heat-to-mechanical energy conversion in combustion engines of gasoline-driven cars is also limited by the efficiency of the Carnot process, η_{HC}, but such engines are not optimized to such a degree as steam turbines, mainly because they operate at a variable shaft speed. Also the maximum value of the torque is sometimes more important than the fuel or energy conversion efficiency. Common values of this efficiency are reported in [24] to be in the range of η_{GV} = 0.18 - 0.20. According to [25] the overall efficiency is about 0.15. The efficiency of 0.20 can be reached with diesel engines, not common in the US.

Comparison of the efficiency of heat-to-mechanical energy conversion in steam turbines and combustion engines is needed here for evaluating the change in the energy demand by a hypothetical replacement of GVs by EVs. This replacement will apply not only to GVs with the highest fuel efficiency, but to gasoline-driven cars with common fuel efficiency. Therefore, for evaluating the change of energy demand with GVs replacement by EVs, an average rather than maximum efficiency η_{GV} is needed. Therefore, assuming that η_{GV} = 0.16, the ratio of efficiencies of combustion engines and steam turbines could be of the order of

$$\frac{\eta_{GV}}{\eta_T} \approx 0.42$$

Since averaging of the efficiency of gasoline-driven cars should go over millions of cars that could be replaced by EVs, and thousands of steam turbines, this ratio has a fixed value. However, it is very difficult to specify it accurately.

3.2.3 Efficiency of Gasoline and Electricity Distribution

Efficiency of gasoline distribution η_{GD} is determined essentially by the amount of gasoline used for its transportation from refineries to gas stations. Average distance and cars used for gasoline transport are the main factors that determine this efficiency. Unfortunately, these data can be evaluated only very roughly. While data on MPG (miles per gallon) of gasoline transporting trucks is available, transporting distances can change in a very wide range. Although there is not specific data to support this number, it seems that gasoline distribution efficiency

$$\eta_{GD} \approx 0.95$$

could be a realistic value.

Efficiency of the electricity distribution is specified by efficiency of power system generators, transformers as well as transmission and distribution lines. Assuming that on average, a synchronous generator of efficiency η_{SG}= 0.98, three transmission transformers of efficiency [26] η_{TT}= 0.99, one distribution transformer of efficiency η_{DT}= 0.98, transmission and sub-transmission lines of efficiency η_{TL}= 0.96; and feeder line of efficiency η_{FL}= 0.98 take a part in energy delivery to residential homes, the efficiency of production and delivery of electric energy could be of the order of

$$\eta_{ED} = \eta_{SG} \times \eta_{TT}^{\,3} \times \eta_{DT} \times \eta_{TL}^{\,2} \times \eta_{FL} = 0.98 \times 0.99^3 \times 0.98 \times 0.96^2 \times 0.98 = 0.88$$

and consequently, the ratio of the gasoline and electricity distribution efficiency could be

$$\frac{\eta_{\mathrm{GD}}}{\eta_{\mathrm{ED}}} \approx 1.08$$

The credibility of this value is not high, but seems to be in accordance with an intuition that distribution of gasoline, meaning its delivery by tank vehicles from refineries to gas stations is quite efficient.

Similar to the efficiency of heat-to-mechanical energy conversion, evaluation of the change of the energy demand with the replacement of GVs by EVs requires that gasoline and electricity distribution efficiencies η_{GD} and η_{ED} over the whole area where this replacement would take place are known. Because of large area of averaging, these efficiencies have fixed, but not well known values.

3.2.4 Electrical Vehicle Efficiency

The system that transfers energy in an EV is made up of four main components. These components are a battery charger, a battery, a DC/AC inverter, and a motor. These subsystems are shown in Fig. 3.3. Resistances in particular subsystems in this figure represent equivalent resistances of these systems with respect to energy losses, ΔW. Consequently, the efficiency of electrical vehicles is not established and can be enhanced with improvement in the car technology.

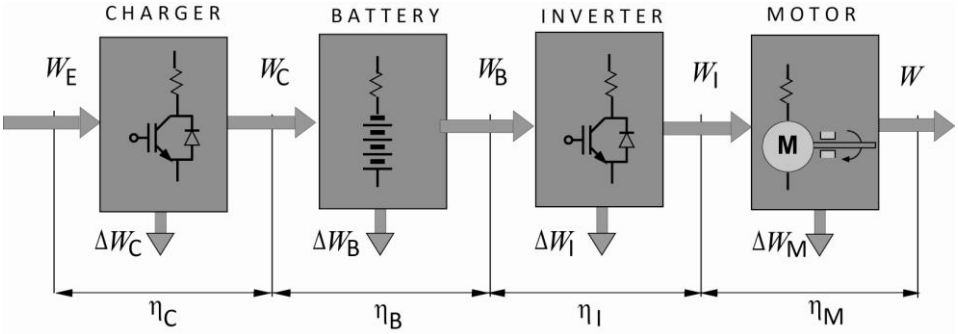

Figure 3.3 Electrical drive subsystems

Electrical motors in EVs are built as permanent magnet synchronous machines (Nissan Leaf and Mitsubishi MiEV) [27] [28] or as variable frequency supplied 3-phase induction machines (Tesla Roadster and Ford Transit Connect Electric) [29] [30]. Manufacturers of EVs do not provide data on the electrical motor efficiency η_M. Only data on general application motors can be found and used for a rough estimation of this value. According to [31] induction motor efficiency can reach a value of 0.95, though η_M = 0.90 is more common. The efficiency of permanent magnet (PM) synchronous machines is typically higher. It increases with the motor power, but PM machines used in EVs are in the medium power range. According to ABB data [32], 370 V, 64kW PM synchronous motor has efficiency 0.93, even if the energy consumed by the cooling system is not included in the efficiency measurement. The efficiency also declines from its maximum value at the motor full load, with the motor load and rotation velocity reduction. Since the average power of an EV motor and its speed of rotation is much lower than their maximum values, the average efficiency of motors used in EVs is probably not higher than η_M = 0.90.

Among batteries of various chemistries, like nickel-metal-hydride or nickel-cadmium, the lithium-ion chemistries currently provide three times higher energy density [33] than other

chemistries. Because of this nearly all recent EVs and PHEVs use lithium-ion batteries. According to manufacturer data efficiency of these batteries is high, but this data is based on measurements of new batteries, and there is a lack of information describing how much this efficiency could decline after many charging cycles. Some amount of energy is dissipated on the battery internal resistance during its charging and discharging. Unfortunately, it is not easy to measure the battery efficiency. Although the energy delivered to the battery can be measured when a car is not used, the energy taken from it depends on the battery current, which changes with driving conditions. Furthermore, the battery cannot be fully discharged to the car motor. Thus, data needed for the battery efficiency calculation is not easily available [34]. The battery efficiency can be calculated by evaluation of energy loss during battery charging and discharging, but battery internal resistance changes with the level of energy storage and battery age. Moreover, the energy loss in a battery changes with the square of the charging or discharging current, and consequently, the efficiency depends on conditions of a battery operation. Based on [35], where results of efficiency measurement, based on calorimetric approach are presented, it can be assumed that $\eta_B = 0.94$. This value is still not very credible, however, since it was measured at cyclic charging and discharging with the same current, while in real situations the discharge current at the motor driving could be much higher than the charging current and internal power loss increases with the square of the current.

To reduce harmonic distortion of the EV supply current, rectifiers needed for battery charging are built [36] [37] as Pulse Width Modulated (PWM) rectifiers. Power transistors switched at a frequency of several kHz and power diodes are the main components of such rectifiers. Power transistors in such devices operate not only in the ON and OFF state, where energy loss is very low, however. When a transistor is switched between ON and OFF states, it

crosses an active region where the loss of energy in the transistor is high. The transistor crosses this area twice in the switching period, and this is the main contribution to energy loss and efficiency degradation. Consequently, PWM rectifiers have much lower energy efficiency η_C as compared to common rectifiers. According to [38] this efficiency can be around 0.92. However, according to [39], at switching frequency of several kHz, it is more likely that this efficiency is closer to $\eta_C = 0.85$.

The inverter needed for conversion of battery DC voltage into a three-phase variable frequency voltage at the motor terminals operates as a three-phase PWM inverter, built of power transistors and switched at a frequency of several kHz. Its efficiency is comparable with that of PWM battery chargers. Thus, we can assume that $\eta_I = \eta_C = 0.85$.

The resultant energy efficiency of EVs is the product of efficiencies of the main subsystems of the car, namely

$$\eta_{EV} = \frac{W}{W_E} = \eta_M \times \eta_I \times \eta_B \times \eta_C \approx 0.90 \times 0.85 \times 0.94 \times 0.85 = 0.61.$$

This value can be challenged by providing more credible values of efficiencies of the car's main power sub-systems.

3.3 Comparison of Energy Required for EVs and GVs

The formula (1) which compares the amount of energy W_{EV} needed for driving an electrical car and energy W_{GV} need for driving a gasoline car which is mechanically identical and in identical conditions, results in the value

$$\frac{W_{EV}}{W_{GV}} = \left(\frac{\eta_{GV}}{\eta_T}\right) \times \left(\frac{\eta_{GD}}{\eta_{ED}}\right) \times \frac{1}{\eta_{EV}} \approx 0.42 \times 1.08 \times \frac{1}{0.61} = 0.74\,.$$

Thus, even if the values of particular efficiencies in this formula are only approximate, this calculation confirms an opinion that electrical cars need less energy than gasoline driven cars. Observe that this formula takes into account the energy lost in steam turbines as well as energy losses in the process of electric energy generation, transmission and distribution.

According to the presented above evaluations, energy savings obtained by replacing GVs with EVs could be around 25%. To obtain a better estimate of energy savings more credible values of energy efficiencies of particular sub-systems are needed. However, it seems clear that EVs are more energy efficient than GVs to some degree.

3.4 EVs Effects on Fossil Fuel Usage and Carbon Emissions

Although some amount of carbon-rich fuel for gasoline cars is provided by bio-fuels, the major sources of this carbon are fossils: crude oil, natural gas, coal, or shale oil. As previously mentioned 69.8% of electricity generated in the U.S. comes from fossil fuels.

Let F_{GV} be the amount of fossils needed for driving a GV, and F_{EV} is the amount of these fossils needed for driving an equivalent EV in the same conditions. Because EVs are supplied partially from plants that do not burn carbon-rich fossils, if a single GV is replaced by an equivalent EV, the demand for fossils changes according to the ratio

$$\frac{F_{\mathrm{EV}}}{F_{\mathrm{GV}}} = \frac{P_{\mathrm{CF}}}{P_{\mathrm{CF}} + P_{\mathrm{NC}}} \times \frac{W_{\mathrm{EV}}}{W_{\mathrm{GV}}}$$

For EVs in the United States, this reduction is approximately equal to

$$\frac{F_{\mathrm{EV}}}{F_{\mathrm{GV}}} = \frac{69.3}{100} \times 0.74 = 0.51\%$$

Thus, each plug-in vehicle which replaces a GV uses only half of the carbon rich fossil fuels. As a result carbon dioxide produced by automobile usage would also be halved. While this is a very rough estimation of the effects of EVs on the national energy and fossil fuels demand and CO_2 emissions, it demonstrates that EVs will very likely reduce fossil fuel consumption and CO2 emissions. These benefits would be further improved by replacing fossil fuel plants with nuclear plants and energy generation facilities using renewables such as wind and solar energy.

CHAPTER 4. MEASUREMENT OF EV BATTERY CHARGING CHARACTERISTICS

4.1 Method of Measurement

To have an idea on the EV battery charging process, measurements of electrical quantities during such charging were performed. The measurements were taken while charging the battery of the Transit Connect Electric, which is not a personal, but a commercial car. At the time of this research, personal EVs like the Nissan Leaf and Chevy Volt were unavailable in Louisiana. Still, the Transit Connect Electric uses similar technology, so these measurements, though not fully representative of the charging process of personal cars, provided relevant information.

Using a Power Monitors Inc. (PMI) Revolution Power Quality Recorder, data from the charging cycle of the EV was recorded. This device was set to record a waveform of voltage and current every ten minutes. Additionally, active power, current RMS, power factor, current harmonics CRMS, and current THD were recorded at one minute intervals. The Revolution monitor takes samples for the measurement of these quantities at a minimum sampling frequency of 250 kHz. During each of these one minute intervals the device stores every sample to temporary memory and uses each sample to compute a min, max, and average value to be recorded at the end of the interval. Since this study is not concerned with instantaneous values, the average is considered the most accurate measurement and is shown in all graphs. The EV battery charger was connected to a 2 x 120 V supply. Two recording channels were used on the monitor, each connected between the neutral and one of the 120 V lines. Therefore, to calculate total active power, the measurements on each should be added together.

4.2 Active Power and Current RMS

An interval graph of active power during the charging cycle is shown in Figure 4.1, and current RMS is shown in Figure 4.2. The graph shows that at the beginning of the charge cycle the charger supplied current around 15 A and active power about 1.8 x 2 = 3.6 kW. During the cycle, charging was paused periodically (approximately every 30 minutes) to evaluate the state of charge of the battery. Once the battery reached around 80% capacity, the current was gradually reduced until it was supplied with half the original charging current. This was done because once 80% capacity is reached, supplying the same current will not charge the battery at the same rate. Rather the extra energy supplied by this current is dissipated as heat and can damage the battery [34]. For the last hour of charging, the charger supplied energy at a rate of about 1.8 kW.

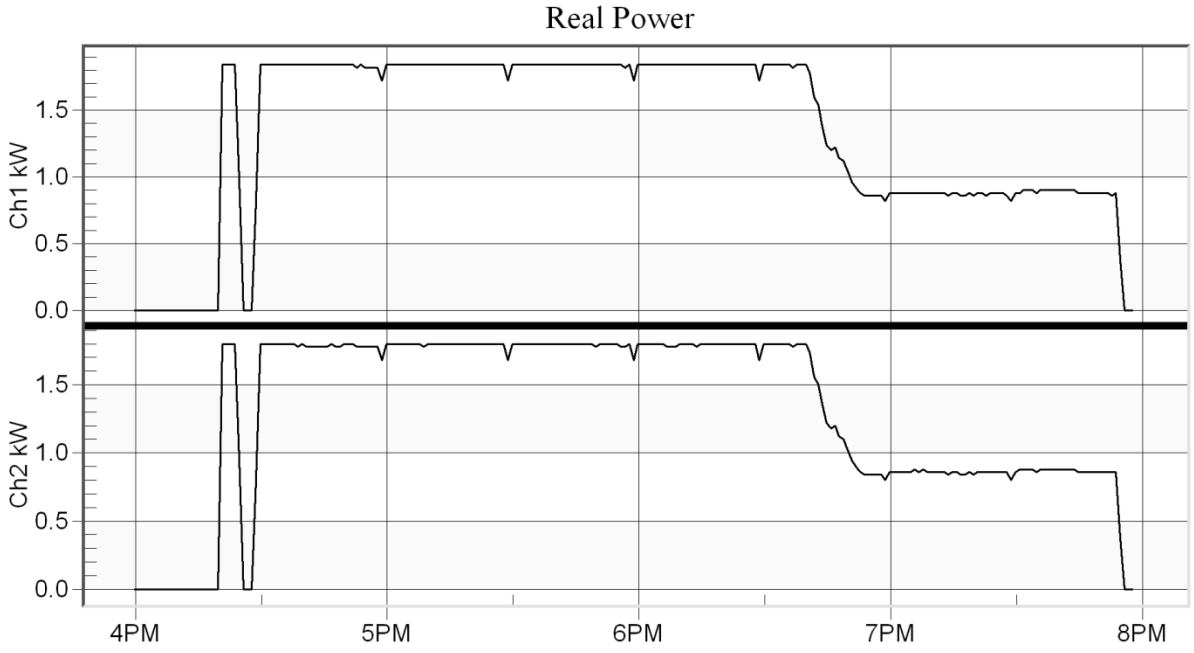

Figure 4.1 Active power during EV battery charging cycle

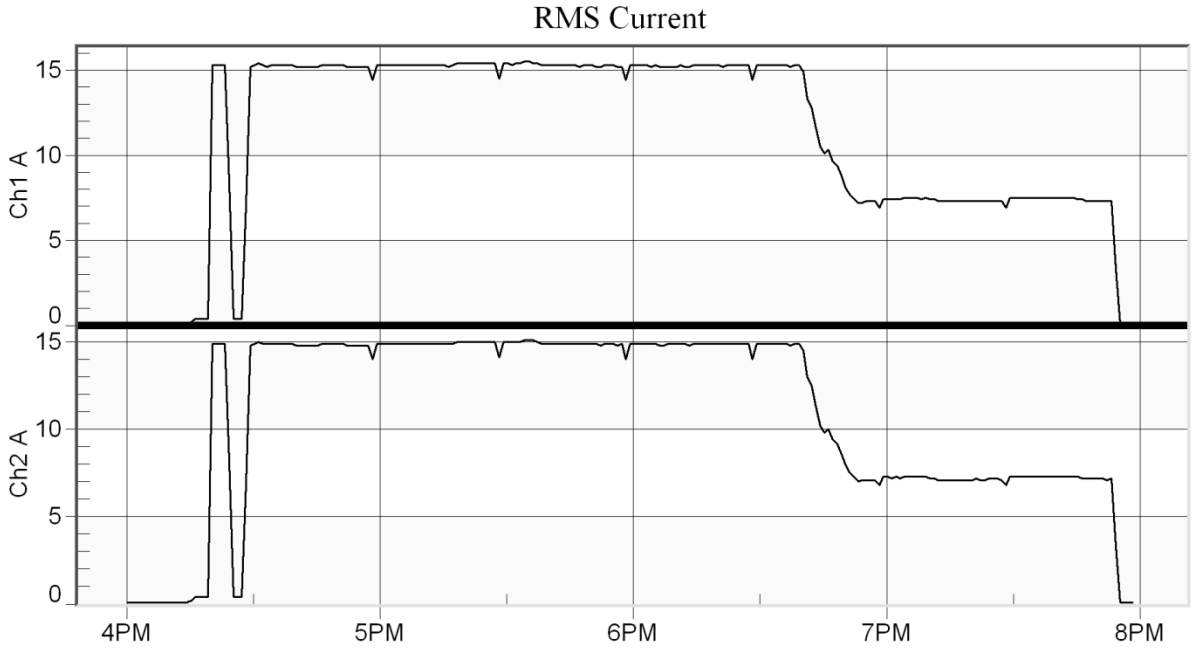

Figure 4.2 Current RMS during EV battery charging cycle

4.3 Power Factor and Current Harmonic Distortion

Voltage and current waveforms during the high current phase of the charging cycle are shown in Figure 4.3. As shown in the figure, the voltage and current were nearly sinusoidal and in phase. This means that harmonic distortion was very low, and the power factor was near unity.

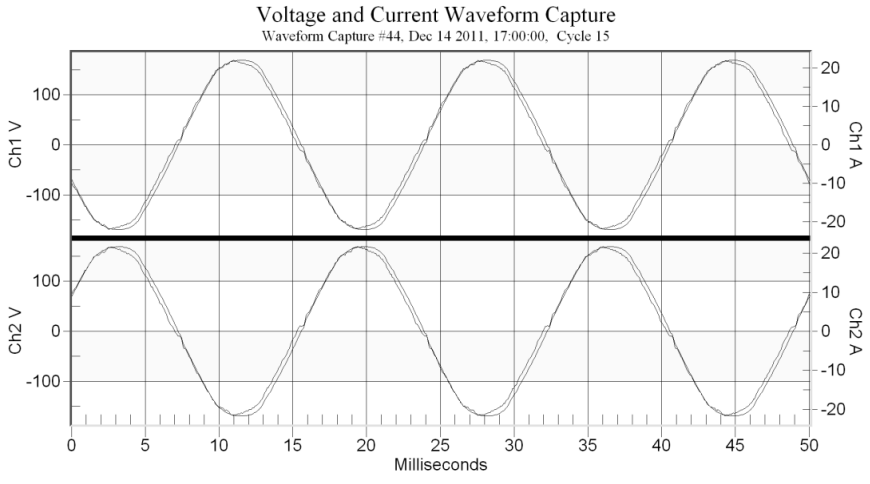

Figure 4.3 Voltage and current waveforms recorded during EV battery charging cycle

Indeed looking at the interval graphs of current THD and power factor, shown in Figures 4.4 and 4.5, it is observed that the current THD was less than 5% for the entire cycle, and the power factor was around 99%. These measurements indicate that the Transit Connect Electric has excellent load characteristics during its charging cycle. In fact, it behaves similar to an ideal resistive load.

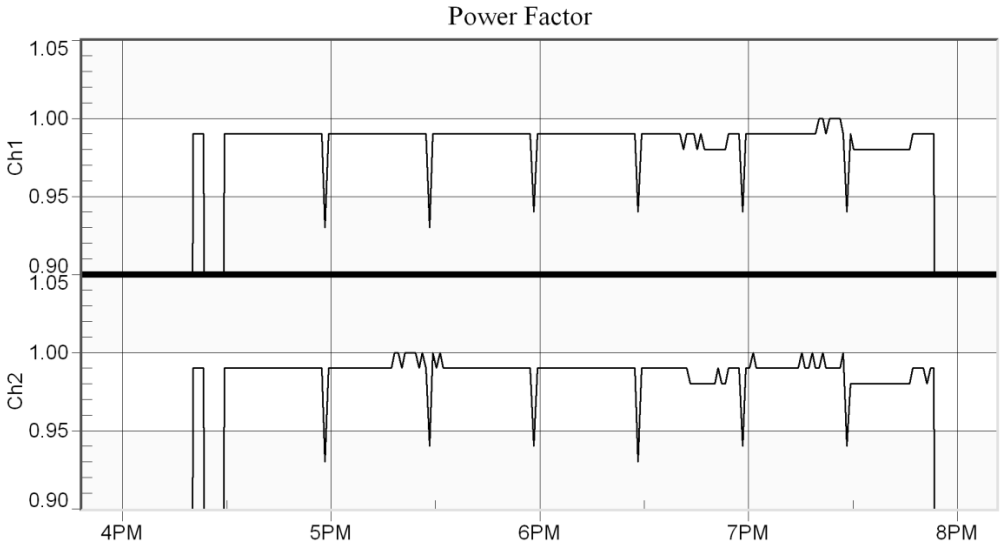

Figure 4.4 Power factor during EV battery charging cycle

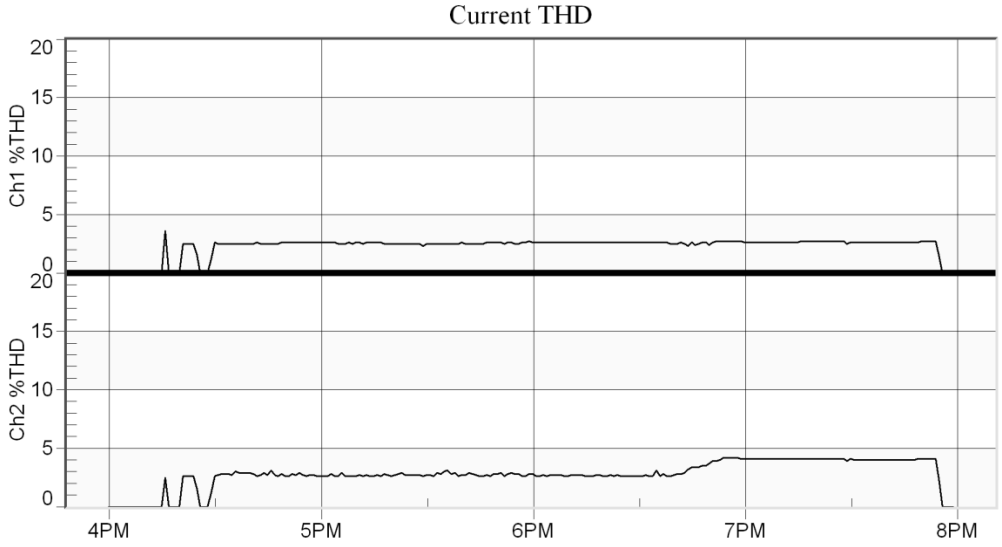

Figure 4.5 Current THD during EV battery charging cycle

4.4 Comparison of Measurements with Standards

IEEE Standard 519-1992 established some limits for current harmonics caused by individual customer loads. The limits depend on the ratio of supply short circuit current to load current. For most distribution systems, loads which draw a current comparable to EV chargers are required to have current distortion less than 15% for odd order harmonics lower than the 11th and a THD no greater than 20%. Also, according to [40], the National Electric Vehicle Infrastructure Working Council requires EV chargers to have a minimum power factor of 95%. The measurements of the Transit Connect Electric show that the current distortion and power factor meet and exceed the standards.

CHAPTER 5. MODELING OF A DISTRIBUTION SYSTEM WITH EV LOADS

5.1 Selected Residential System for Modeling

To investigate the effects of EV battery chargers on residential distribution systems, modeling and analysis of an actual distribution system was performed. The selected system supplies energy to the English Turn neighborhood in New Orleans, where the average home price in 2010 was around three times the national average [41] [42]. The people living in such an expensive neighborhood would likely be able to afford an EV even at their current high prices. Therefore, this kind of neighborhood could see higher EV penetration sooner than others.

The selected residential system data was provided by Entergy, the power utility company that serves most of the residents in the area. According to this data, there are 837 customers served by this feeder which is a radial network. Typically, voltage harmonic distortion problems occur in more localized areas such as a group of loads connected to the same node of a single-phase system. A large load which causes high current harmonic distortion in such a system could cause excessive voltage distortion to occur. Therefore, harmonic analysis of the system was focused on a few homes connected to residential transformers on a single phase to observe the effects of each individual customer. All other loads were modeled as lumped loads, and their load characteristics were estimated based on given general system data.

5.2 System Elements and Topology

A one-line diagram of the distribution system provided by Entergy is shown in Figure 5.1. This system is redrawn as a simplified circuit in Figure 5.2 with each node used for nodal analysis labeled. Some approximations were made in this simplified circuit. All loads other than the homes connected to the single phase conductor on the one-line diagram are represented as two

lumped loads at nodes 1 and 2. The total demand of all customers from the substation to node 1 on all three phases is

$$S'_{L1,3Ph} = 8.965 - 4.642 = 4.3\ MVA$$

Assuming that the loads are evenly distributed on the three phases, the demand on a single phase would be

$$S'_{L1} = \frac{S_{T1}}{3} = \frac{4.323}{3} = 1.4\ MVA$$

Using the same assumption, the total demand of all loads on a single phase between nodes 1 and 2 is

$$S'_{L2} = \frac{4.642}{3} - 0.096 = 1.5\ MVA$$

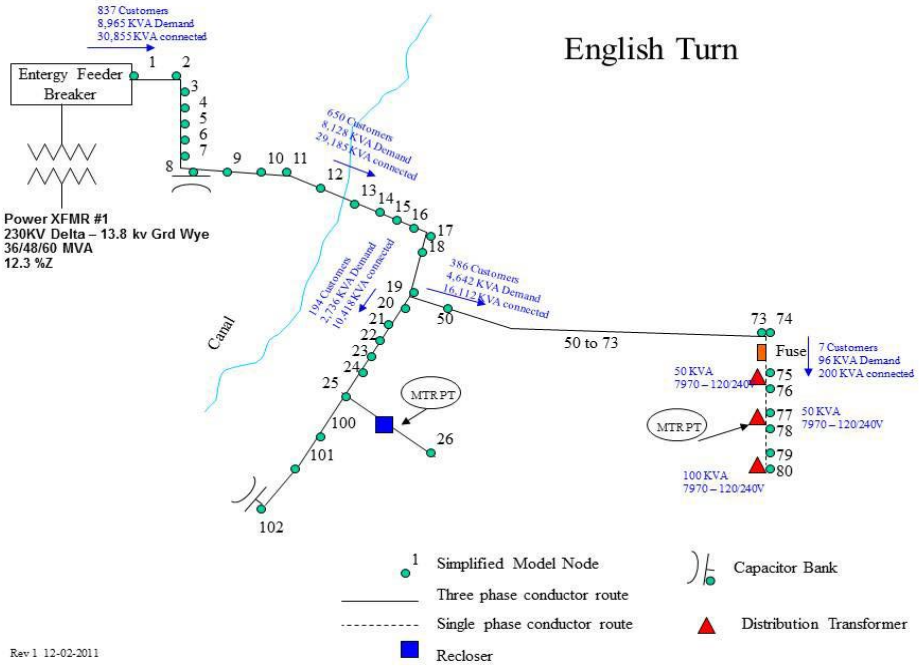

Figure 5.1 One-line diagram of selected residential system

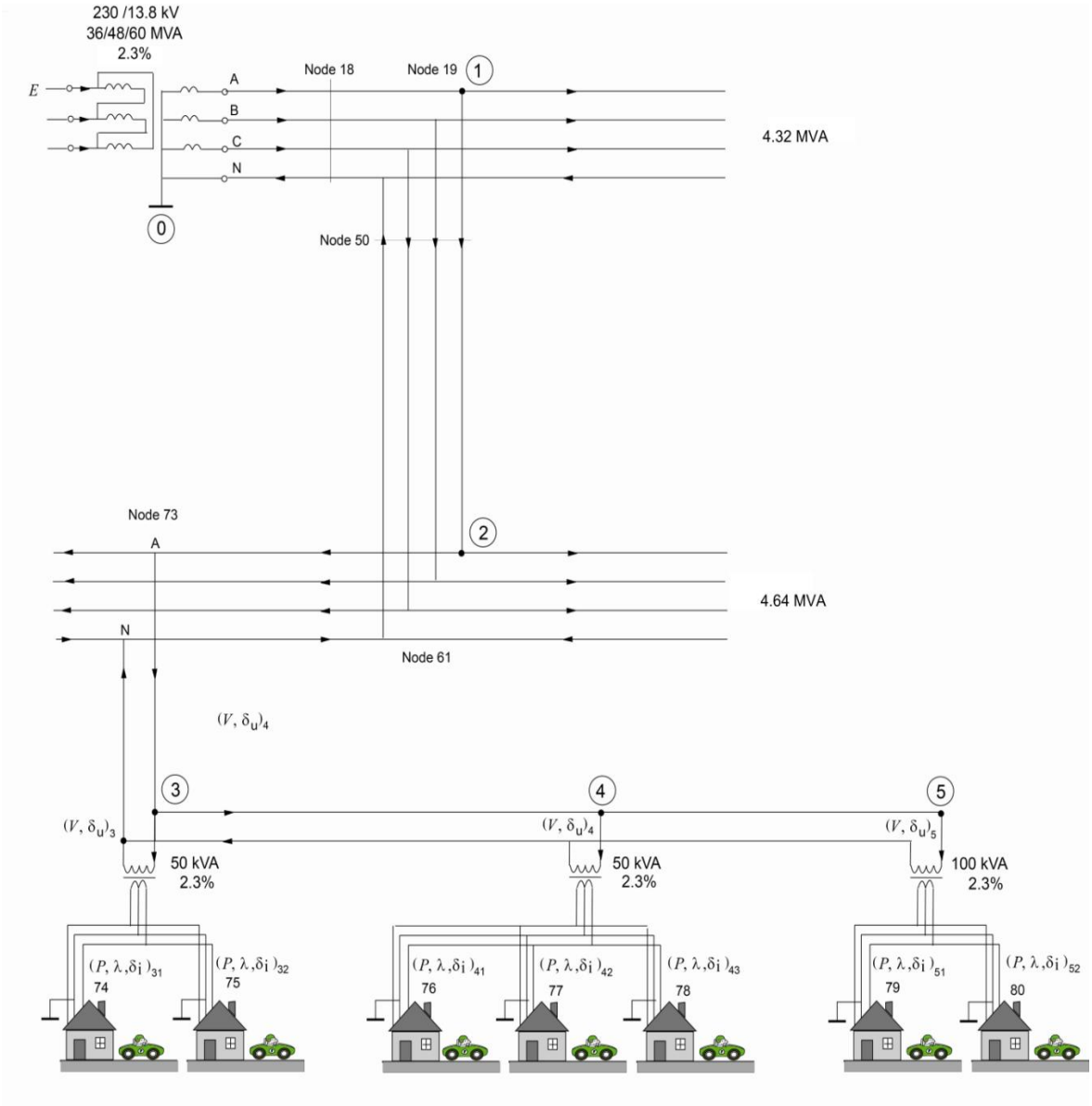

Figure 5.2 Simplified diagram of residential system

5.3 Method of Analysis

The system load and line admittances were calculated for the fundamental harmonic. After obtaining these admittances, nodal analysis was performed using the system admittance matrix and the matrix of injected currents into the nodes to obtain voltage and current fundamental harmonic values of the whole system. Using the current fundamental values and

some data describing the load harmonic distribution, the current harmonics generated by the loads for each harmonic order were calculated.

Nodal analysis was repeated for each harmonic frequency to obtain the CRMS values of the voltage harmonics at each node which are used to calculate the voltage RMS and total harmonic distortion (THD). Harmonics calculation was done with a computer model coded in Matlab, and then calculations were done manually for the fundamental and third harmonic to verify the results. This process of hand calculation is described in Sections 5.4 ~5.7. It should be noted that all computed values reported are rounded to two significant figures. Since repeated rounding accumulates error, the hand calculation was actually performed using five significant figures.

5.4 Calculating Circuit Model Parameters for Fundamental Harmonic

5.4.1 Circuit Model Using Traditional Circuit Elements

The distribution system shown in Figure 5.2 was modeled for the first harmonic using traditional circuit elements as shown in Figure 5.3. Each home on the single phase feeder was modeled as an admittance element, and all other homes were modeled as lumped admittances at the end of the distribution line. The distribution lines and transformers were modeled as inductive impedance elements. The system was assumed to be supplied by a symmetrical infinite bus, and the loads on the system were assumed to be equally distributed on each phase. The calculation of the impedances and admittances of these circuit elements is explained in the following subsections.

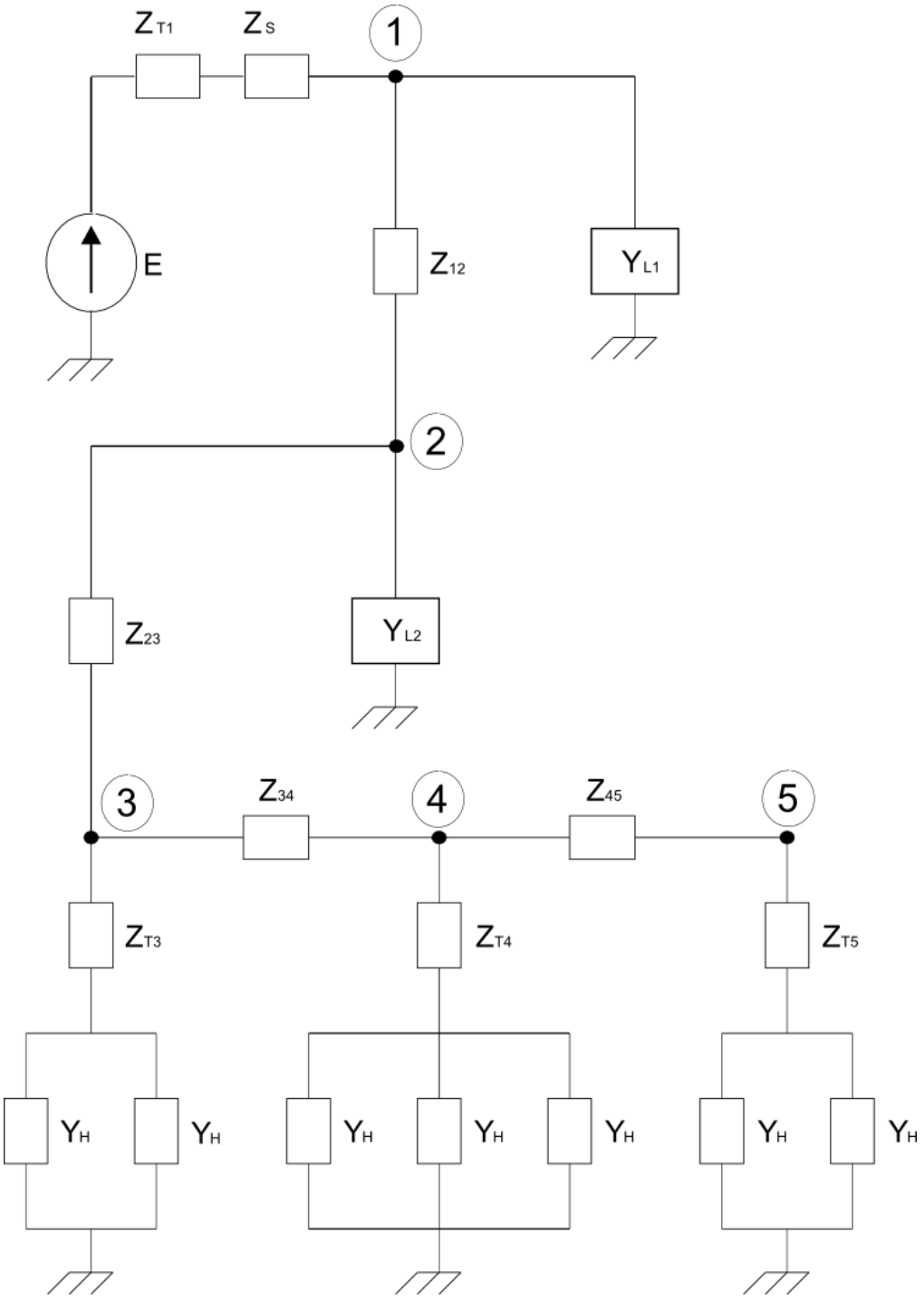

Figure 5.3 Single-phase circuit model of residential system

5.4.2 Per-Unit System

To simplify calculations the per-unit system was used. Figure 5.4 shows the circuit model separated into three sections labeled A, B, and C. These sections are all the parts of the circuit supplied with the same nominal voltage, and thus, the transformers separate each section.

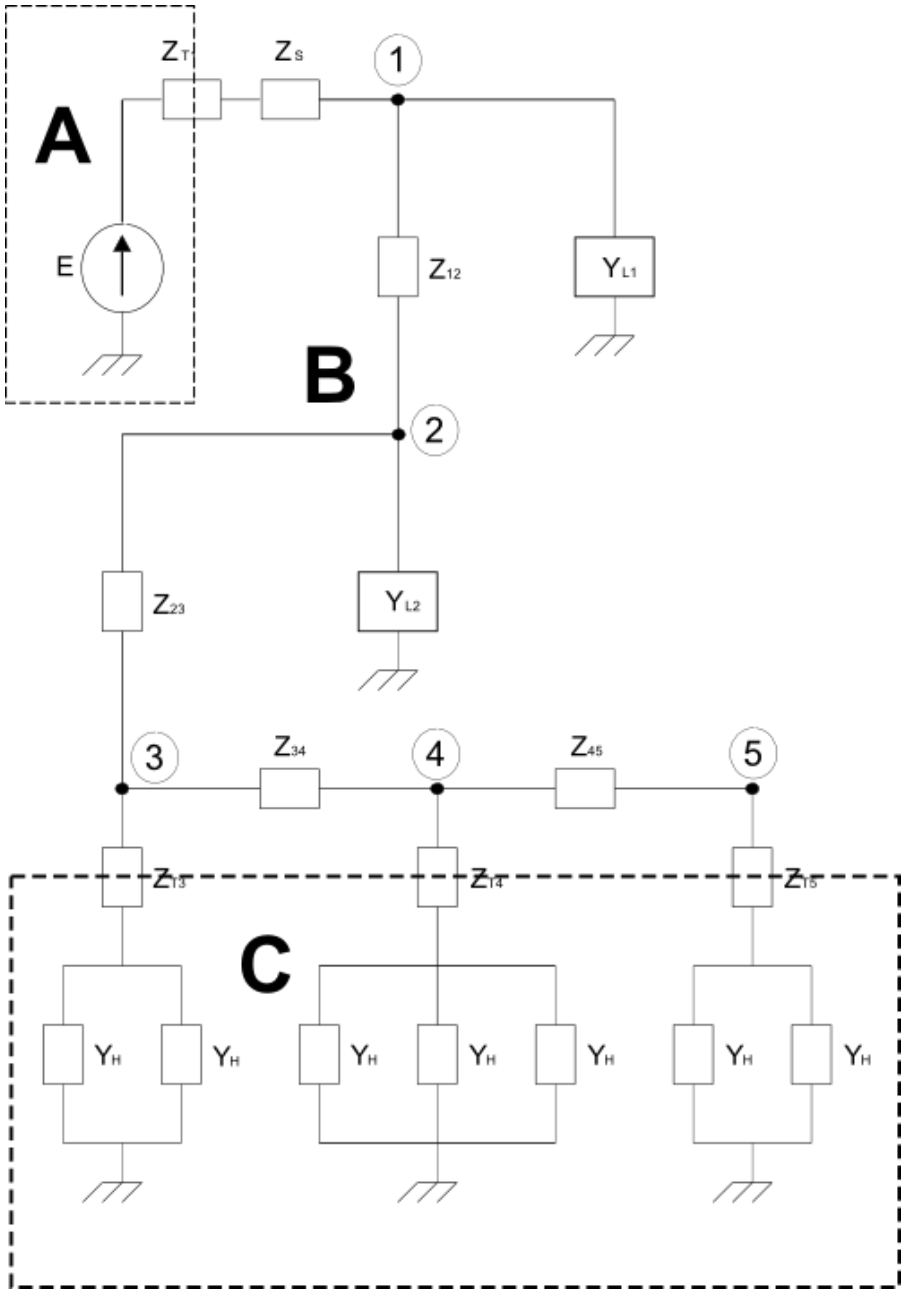

Figure 5.4 Circuit divided into sections based on nominal voltage

The bases chosen for each section are shown in Table 5.1. The voltage bases were chosen as the nominal line-to-neutral voltages. The apparent power base was chosen to be equal to the MVA rating of the substation transformer. As a convention, in this thesis the symbol *K* is used to represent a base value. The subscript specifies the type of base. For instance K_I, K_S, and K_V are base current, apparent power, and voltage respectively. Base currents were calculated by

$$K_I = \frac{K_S}{K_V},$$

Base impedance is given by

$$K_Z = \frac{K_V^2}{K_S}.$$

Table 5.1 Base table used for per-unit analysis

$K_S = 36\ MVA$			
	Section A	**Section B**	**Section C**
K_V	130 kV	7970 V	120 V
K_I	270 A	4.5 kA	300 kA
K_Z	490 Ω	1.8 Ω	0.4 mΩ

Using these bases, the per-unit values of all quantities are given by the relation

$$x = \frac{x'}{K_x}$$

By using this system the transformer impedances and the impedances of any connected loads do not need to be recalculated to the primary or secondary for analysis. Instead all values found by analysis will be per-unit quantities which can then be converted to the actual values by

multiplying by the proper base. Note that in this thesis variables with an apostrophe are actual values, while the symbols without an apostrophe are in per-unit.

5.4.3 Transformer Impedances Calculation

There were four transformer impedances in the system to be calculated. They are labeled in Figure 5.2 as $\boldsymbol{Z}_{T1}, \boldsymbol{Z}_{T2}, \boldsymbol{Z}_{T3}$, and $\boldsymbol{Z}_{T4}$. The first transformer is a 230/13.8kV transformer in the distribution substation. The other three are single-phase, 7970/120V transformers which supply two or three homes each. The home transformers actually have a 2 x 120 V secondary capable of supplying a total of 240 V, but for simplicity the transformers are modeled as having only a 120 V secondary. The rated per-unit impedance magnitudes and apparent power ratings were provided by Entergy and are shown previously in Figure 5.1. These given per-unit impedances use the nominal apparent power of each transformer as the base. For all but the substation transformer, these apparent power bases are different from the K_S of the distribution system, so they must be converted to a new per-unit impedance. The converted impedance magnitude of a single phase transformer is given by

$$Z_T = \left(\frac{K_{V,rat}}{K_V}\right)^2 \times \frac{K_S}{K_{S,rat}} \times Z_{T,rat}$$

Where $K_{V,rat}$, $K_{S,rat}$, and $Z_{T,rat}$ are the rated values given by the utility company, and the other base values are the ones shown in Table 5.1. Since the rated base voltage $K_{V,rat}$ is the same base used for per-unit analysis of this section of the circuit, the formula simplifies to

$$Z_T = \frac{K_S}{K_{S,rat}} \times Z_{T,rat}$$

The transformers on nodes 3 and 4 both have a nominal kVA rating of 50 kVA and impedance rating of 2.3%. Therefore the recalculated per-unit impedance is

$$Z_{T3} = Z_{T4} = \frac{K_S}{K_{S3,rat}} \times Z_{T3,rat} = \frac{36 \times 10^6}{50 \times 10^3} \times 0.023 = 17\ pu$$

The transformer on node 5 also has an impedance rating of 2.3%, but the nominal kVA rating is 100 kVA. The recalculated per-unit impedance of this transformer is

$$Z_{T5} = \frac{K_S}{K_{S5,rat}} \times Z_{T5,rat} = \frac{36 \times 10^6}{100 \times 10^3} \times 0.023 = 8.3\ pu$$

To obtain the resistance and reactance of the transformers their X/R ratio must be known. From IEEE Standard C37.010, the typical X/R ratio for the three-phase transformer in this system is around 28, while the other transformers have a typical X/R ratio of 10. Using the typical X/R ratio, the resistance and reactance of the transformer at node *m* is given by

$$R_{Tm} = \frac{Z_{Tm}}{\sqrt{1 + \sigma_{Tm}^2}}$$

$$X_{Tm} = \sigma_{Tm} R_{Tm},$$

where σ_{Tm} is the transformer X/R ratio. Applying these equations to the transformer at node 3, the resistance and reactance are

$$R_{T3} = \frac{Z_{T3}}{\sqrt{1 + \sigma_{T3}^2}} = \frac{17}{\sqrt{1 + 10^2}} = 1.7\ pu$$

$$X_{T3} = \sigma_{T3} R_{T3} = 10 \times 1.7 = 17\ pu.$$

The impedance would then be

$$\boldsymbol{Z}_{T3} = R_{T3} + jX_{T3} = 1.7 + j17\ pu.$$

The transformer at node 4 is identical to the one at node 3, so its impedance is the same.

$$\boldsymbol{Z}_{T4} = \boldsymbol{Z}_{T3} = 1.7 + j17\ pu$$

The calculation for the transformer impedance at node 5 is done in the same way.

$$R_{T5} = \frac{Z_{T5}}{1 + \sigma_{T5}^2} = \frac{8.28}{1 + 10^2} = 0.82\ pu$$

$$X_{T5} = \ \sigma_{T5} R_{T5} = 10 \times 0.82 = 8.2\ pu$$

$$\boldsymbol{Z}_{T5} = R_{T5} + jX_{T5} = 0.82 + j8.2\ pu$$

The resistance and reactance of the substation transformer could also be computed using the X/R ratio, but since X/R is 28 for this transformer, to simplify hand calculations the substation transformer can be considered as purely inductive. This means the substation transformer reactance is

$$X_{T1} = Z_{T1} = 0.023\ pu$$

And the impedance is

$$\boldsymbol{Z}_{T1} = jX_{T1} = j0.023\ pu.$$

5.4.4 Lumped Load Admittances Calculation

As shown in Figure 5.3, there are two lumped loads in the circuit model. For the lumped load at node 1 the demand was found in Section 5.2 to be

$$S'_{L1} = 1.4\ MVA.$$

This apparent power converted to per-unit would be

$$S_{L1} = \frac{S'_{L1}}{K_S} = \frac{1.4}{36} = 0.040\ pu$$

If the load power factor is known, the load admittance can be obtained. From Entergy's system data, a typical value of power factor for these loads would be

$$\lambda_{L1} = 0.87$$

The active power of the lumped load would then be given by

$$P_{L1} = S_{L1}\lambda_{L1} = 0.040 \times 0.87 = 0.035\ pu$$

Assuming that $V'_{L1} = K_V$, the conductance is

$$G_{L1} = \frac{P_{L1}}{\left(\frac{V'_{L1}}{K_V}\right)^2} = \frac{P_{L1}}{1^2} = P_{L1} = 0.035\ pu$$

The reactive power is given by

$$Q_{L1} = S_{L1}\sin(\cos^{-1}(\lambda_{L1})) = 0.040 \times \sin\ cos^{-1}\ 0.87 = 0.020pu$$

Again assuming that $V'_{L1} = K_V$, susceptance is given by

$$B_{L1} = -\frac{Q_{L1}}{\left(\frac{V'_{L1}}{K_V}\right)^2} = -\frac{Q_{L1}}{1^2} = -Q_{L1} = -0.020\ pu$$

So the total admittance of the lumped load at node 1 is

$$\boldsymbol{Y}_{L1} = G_{L1} + jB_{L1} = 0.035 - j0.020\ pu$$

Calculation of the admittance of the lumped load at node 2 follows the same procedure using the given demand for that load.

$$S'_{L2} = 1.5\ MVA$$

$$S_{L2} = \frac{S'_{L2}}{B_S} = \frac{1.45}{36} = 0.040\ pu$$

As the previous equation shows, S_{L2} is approximately equal to S_{L1}. Assuming the same power factor, the admittance would then be approximately the same.

$$\boldsymbol{Y}_{L2} \cong \boldsymbol{Y}_{L1} = 0.035 - j0.020\ pu$$

5.4.5 Home Admittances Calculation

As shown in Figure 5.2, there are up to three homes connected in parallel to each single-phase transformer. Each of these homes will be modeled as a passive inductive load for the fundamental harmonic. A typical active power for a home in this area is

$$P'_H = 2.5\ kW.$$

Converting to per-unit this power is

$$P_H = \frac{P'_H}{K_S} = \frac{2.5 \times 10^3}{36 \times 10^6} = 6.9 \times 10^{-5}\ pu.$$

Assuming that the home voltage, V'_H is equal to the base voltage, equivalent conductance of each home is given by

$$G_H = \frac{P_H}{\frac{V'_H}{K_V}^2} = \frac{P_H}{1^2} = P_H = 6.9 \times 10^{-5}\ pu.$$

A typical power factor chosen for these homes is

$$\lambda_H = 0.87.$$

Then reactive power can be obtained by

$$Q_H = P_H \tan(\cos^{-1}(\lambda_H)) = 6.9 \times 10^{-5} \times \tan\ \cos^{-1}\ 0.87 \quad = 3.9 \times 10^{-5}\ pu.$$

Thus, the equivalent susceptance is given by

$$B_H = -\frac{Q_H}{\frac{V'_H}{K_V}^2} = -\frac{Q_H}{1^2} = -Q_H = -3.9 \times 10^{-5}\ pu.$$

And the equivalent admittance of a home is

$$\boldsymbol{Y}_H = G_H + jB_H = \ \ 6.9 - j3.9\ \ \times 10^{-5}\ pu.$$

5.4.6 Distribution Line Impedances Calculation

According to Entergy's system data, most of the three-phase lines used in this system were 954,000 cmil, 37-strand, all-aluminum conductor (AAC) with a given impedance per mile rating at one foot spacing of

$$\frac{\boldsymbol{Z}'_{AAC}}{l_{AAC}} = (0.0905 + j0.404)\frac{\Omega}{mi}$$

There was also a significant length of insulated copper cable that was underground below a canal. This type of cable will be referred to as C cable. This line had an impedance per mile rating at one foot spacing of

$$\frac{\boldsymbol{Z'}_C}{l_C} = (0.02528 + j0.0898)\frac{\Omega}{mi}$$

The line lengths from the substation transformer to node 1 are shown in Table 5.2.

Table 5.2 Substation to node 1 line lengths, *C cable

Substation to Node 1 Line Lengths		
Point From	Point To	Line Length (ft)
1	2	254
2	3	25
3	4	317
4	5	169
5	6	524
6	7	269
7	8	2224
8	9	398
9	10	184
10	11	432
11	12	24
12	13	*1235
13	14	16
14	15	89
15	16	350
16	17	1087
17	18	506
18	19	141
Total Length of AAC		7009
Total Length of C		1235

The total impedance of the line from the substation to node 1 was found by

$$\boldsymbol{Z'}_s = \frac{\boldsymbol{Z'}_{AAC}}{l_{AAC}} \times \frac{l_{s,AAC}}{5280} + \frac{\boldsymbol{Z'}_C}{l_C} \times \frac{l_{s,C}}{5280}$$

$$= \ 0.0905 + j0.404 \ \times \frac{7009}{5280} + \ 0.02528 + j0.0898 \ \times \frac{1235}{5280}$$

$$= (0.13 + j0.56)\Omega$$

where $l_{s,AAC}$ and $l_{s,C}$ are the length of the AAC and C type cable respectively between the substation and node 1 in feet.

Between nodes 1 and 2 the conductor was entirely AAC. The lengths of the lines in this section are shown in Table 5.3.

Table 5.3 Node 1 to node 2 line lengths

Node 1 to Node 2 Line Lengths		
Point From	Point To	Line Length (ft)
19	50	13
50	51	757
51	52	564
52	53	244
53	54	193
54	55	964
55	56	288
56	57	967
57	58	202
58	59	196
59	60	197
60	61	669
Total Length of AAC		5254

The total impedance between nodes 1 and 2 was found by

$$\boldsymbol{Z'}_{12} = \frac{\boldsymbol{Z'}_{AAC}}{l_{AAC}} \times \frac{l_{12,AAC}}{5280} = \ 0.0905 + j0.404 \ \times \frac{5254}{5280} = (0.090 + j0.40)\Omega$$

Most of the line between nodes 2 and 3 was the same AAC conductor. However, at the end of the line it was AWG #2 copper conductor (CU). This conductor had a given impedance per mile rating at one foot spacing of

$$\frac{\boldsymbol{Z}'_{CU}}{l_{CU}} = (0.887 + j0.5227)\frac{\Omega}{mi}$$

The line lengths between node 2 and 3 are given in Table 5.4.

Table 5.4 Node 2 to node 3 line lengths

Node 2 to Node 3 Line Lengths		
Node From	Node To	Line Length (ft)
61	62	94
62	63	24
63	64	259
64	65	858
65	66	725
66	67	1019
67	68	1015
68	69	226
69	70	476
70	71	24
71	72	168
72	73	211
73	74	4
Total Length of AAC		5103
74	75	240
75	76	125
Total Length of CU		365

The total impedance of the line was found by

$$\boldsymbol{Z'}_{23} = \frac{\boldsymbol{Z'}_{AAC}}{l_{AAC}} \times \frac{l_{23,AAC}}{5280} + \frac{\boldsymbol{Z'}_{CU}}{l_{CU}} \times \frac{l_{23,CU}}{5280}$$

$$= \ 0.0905 + j0.404 \ \times \frac{5103}{5280} + (0.887 + j0.5227) \times \frac{365}{5280} = (0.15 + j0.43)\Omega$$

Between nodes 3 and 4 the conductor was entirely CU. The lengths of the lines in this section are shown in Table 5.5.

Table 5.5 Node 3 to node 4 line lengths

Node 3 to Node 4 Line Lengths		
Node From	Node To	Line Length (ft)
76	77	156
77	78	38
Total Length of CU		194

The total impedance between nodes 3 and 4 was found by

$$\boldsymbol{Z'}_{34} = \frac{\boldsymbol{Z'}_{CU}}{l_{CU}} \times \frac{l_{34,CU}}{5280} = (0.887 + j0.5227) \times \frac{194}{5280} = (0.033 + j0.019)\Omega$$

Between nodes 4 and 5 the conductor was all CU as well. Table 5.6 shows the line lengths.

Table 5.6 Node 4 to node 5 line lengths

Node 4 to Node 5 Line Lengths		
Node From	Node To	Line Length (ft)
78	79	363
79	80	86
Total Length of CU		449

The total impedance between nodes 4 and 5 was found by

$$\boldsymbol{Z'}_{45} = \frac{\boldsymbol{Z'}_{CU}}{l_{CU}} \times \frac{l_{45,CU}}{5280} = (0.887 + j0.5227) \times \frac{449}{5280} = (0.075 + j0.044)\Omega$$

The per-unit impedances of the lines were then computed using the base for Section B from Table 5.1.

$$\boldsymbol{Z}_s = \frac{\boldsymbol{Z'}_s}{K_Z} = \frac{0.13 + j0.56}{1.8} = 0.070 + j0.31\ pu$$

$$\boldsymbol{Z}_{12} = \frac{\boldsymbol{Z'}_{12}}{K_Z} = \frac{0.090 + j0.40}{1.8} = 0.050 + j0.22\ pu$$

$$\boldsymbol{Z}_{23} = \frac{\boldsymbol{Z'}_{23}}{K_Z} = \frac{0.15 + j0.43}{1.8} = 0.083 + j0.24\ pu$$

$$\boldsymbol{Z}_{34} = \frac{\boldsymbol{Z'}_{34}}{K_Z} = \frac{0.033 + j0.019}{1.8} = 0.018 + j0.011\ pu$$

$$\boldsymbol{Z}_{45} = \frac{\boldsymbol{Z'}_{45}}{K_Z} = \frac{0.075 + j0.044}{1.8} = 0.042 + j0.025\ pu$$

5.5 Nodal Analysis for Fundamental Harmonic

5.5.1 Equivalent Circuit for Nodal Analysis

Once all parameters in the equivalent circuit model shown in Figure 5.3 were obtained, the circuit was redrawn to the form required for nodal analysis as shown in Figure 5.5. As shown in the figure, at node 1 the lumped load, transformer, and distribution line were all combined into one node admittance in parallel with a current source which is the Norton equivalent. The homes and the transformers they were connected to at each node were combined into one node admittance. Additionally, the distribution line impedances were converted to admittances. This

equivalent circuit is in the correct form to create a system admittance matrix and current matrix to solve for node voltages. This section details the calculation of the parameters in this equivalent circuit and using the admittance matrix to solve for node voltages. It should be noted that in this circuit $\boldsymbol{Y}_2$ is the same as $\boldsymbol{Y}_{L2}$ which was calculated in Section 5.4.4.

$$\boldsymbol{Y}_2 = \boldsymbol{Y}_{L2} = 0.035 - j0.020\ pu$$

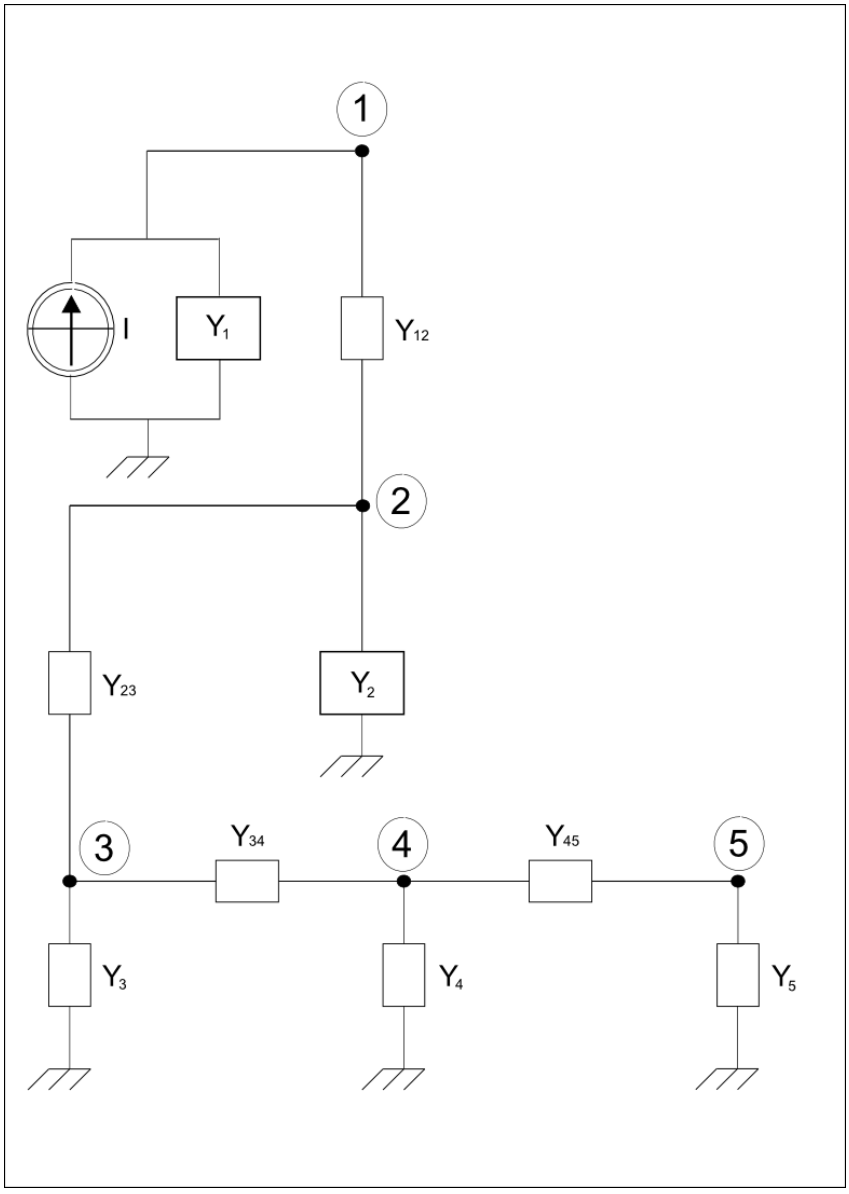

Figure 5.5 Single-phase circuit model redrawn for nodal analysis

5.5.2 Calculating Norton Equivalent of Circuit at Node 1

As shown in Figure 5.3, $\boldsymbol{Z}_s$ is connected in series with $\boldsymbol{Z}_{T1}$. These impedances were combined into an equivalent impedance.

$$\boldsymbol{Z}_{E1} = \boldsymbol{Z}_s + \boldsymbol{Z}_{T1} = 0.070 + j0.31 + j0.023 = 0.070 + j0.33\ pu$$

This impedance in series with the voltage source was transformed to an admittance in parallel with a current source.

$$\boldsymbol{Y}_{E1} = \frac{1}{\boldsymbol{Z}_{E1}} = \frac{1}{0.070 + j0.33} = 0.61 - j2.9 = 3.0e^{-j78^{\circ}} pu$$

$$I = E \times Y_{E1} = 1 \times 3.0 = 3.0\ pu$$

The equivalent admittance, $\boldsymbol{Y}_{E1}$ is in parallel with the lumped load admittance, $\boldsymbol{Y}_{L1}$. These two admittances were summed to obtain the equivalent node 1 admittance.

$$\boldsymbol{Y}_1 = \boldsymbol{Y}_{E1} + \boldsymbol{Y}_{L1} = 0.61 - j2.9 + 0.035 - j0.020 = 0.65 - j2.9\ pu$$

5.5.3 Calculating Equivalent Admittances at Nodes 3, 4, and 5.

As shown in Figure 5.3, the home loads connected to each transformer are connected in parallel. They were combined into equivalent admittances by summing each connected home admittance. Let H_m be the total number of homes on transformer *m*. Since each home is assumed to be the same, the equivalent admittance is given by

$$\boldsymbol{Y}_{Em} = H_m \times Y_H$$

For node 3:

$$H_3 = 2$$

$$\boldsymbol{Y}_{E3} = H_3 \times \boldsymbol{Y}_H = 2 \times \ 6.9 - j3.9 \ \times 10^{-5} = \ 13.9 - j7.9 \ \times 10^{-5}\ pu.$$

The equivalent impedance is

$$\boldsymbol{Z}_{E3} = \frac{1}{\boldsymbol{Y}_{E3}} = \frac{1}{14.0 - j7.9 \ \times 10^{-5}} = 5400 + j3100\ pu.$$

For node 4:

$$H_4 = 3$$

$$\boldsymbol{Y}_{E4} = H_4 \times \boldsymbol{Y}_H = 3 \times \ 6.9 - j3.9 \ \times 10^{-5} = \ 21 - j12 \ \times 10^{-5}\ pu.$$

The equivalent impedance is

$$\boldsymbol{Z}_{E4} = \frac{1}{\boldsymbol{Y}_{E4}} = \frac{1}{21 - j12 \ \times 10^{-5}} = 3600 + j2100\ pu.$$

Node 5 has two houses just like node 3. Therefore the equivalent impedance is the same.

$$\boldsymbol{Z}_{E5} = \boldsymbol{Z}_{E3} = 5400 + j3100\ pu$$

These equivalent impedances are in series with the single-phase transformer impedances, so they were combined into equivalent node impedances. Having these impedances, the node admittances were found for use in the admittance matrix.

For node 3:

$$\boldsymbol{Z}_3 = \boldsymbol{Z}_{E3} + \boldsymbol{Z}_{T3} = 5400 + j3100 + 1.7 + j17 = 5500 + j3100\ pu$$

$$\boldsymbol{Y}_3 = \frac{1}{\boldsymbol{Z}_3} = \frac{1}{5400 + j3100} = (1.4 - j0.79) \times 10^{-4}\ pu$$

For node 4:

$$\boldsymbol{Z}_4 = \boldsymbol{Z}_{E4} + \boldsymbol{Z}_{T4} = 3600 + j2100 \ + 1.7 + j17 = 3600 + j2100 \, pu$$

$$\boldsymbol{Y}_4 = \frac{1}{\boldsymbol{Z}_4} = \frac{1}{3600 + j2100} = \ 2.1 - j1.2 \ \times 10^{-4} \, pu$$

For node 5:

$$\boldsymbol{Z}_5 = \boldsymbol{Z}_{E5} + \boldsymbol{Z}_{T5} = 5400 + j3100 \ + 0.82 + j8.2 = 5500 + j3100 \, pu$$

$$\boldsymbol{Y}_5 = \frac{1}{\boldsymbol{Z}_5} = \frac{1}{5500 + j3100} = \ 1.4 - j0.79 \ \times 10^{-4} pu$$

5.5.4 Calculating Line Admittances

The line admittances were calculated by taking the reciprocal of the line impedances.

$$\boldsymbol{Y}_s = \frac{1}{\boldsymbol{Z}_s} = \frac{1}{0.070 + j0.31} = 0.70 - 3.1 \, pu$$

$$\boldsymbol{Y}_{12} = \frac{1}{\boldsymbol{Z}_{12}} = \frac{1}{0.05 + j0.22} = 0.96 - j4.3 \, pu$$

$$\boldsymbol{Y}_{23} = \frac{1}{\boldsymbol{Z}_{23}} = \frac{1}{0.083 + j0.24} = 1.3 - j3.8 \, pu$$

$$\boldsymbol{Y}_{34} = \frac{1}{\boldsymbol{Z}_{34}} = \frac{1}{0.018 + j0.012} = 41 - j24 \, pu$$

$$\boldsymbol{Y}_{45} = \frac{1}{\boldsymbol{Z}_{45}} = \frac{1}{0.042 + j0.025} = 18 - j10 \, pu$$

5.5.5 Using Admittance Matrix for Fundamental Harmonic Nodal Analysis

The admittance matrix was constructed using the following form.

$$\mathbf{Y} = \begin{bmatrix} Y_1 + Y_{12} & -Y_{12} & 0 & 0 & 0 \\ -Y_{12} & Y_2 + Y_{12} + Y_{23} & -Y_{23} & 0 & 0 \\ 0 & -Y_{23} & Y_3 + Y_{23} + Y_{34} & -Y_{34} & 0 \\ 0 & 0 & -Y_{34} & Y_4 + Y_{34} + Y_{45} & -Y_{45} \\ 0 & 0 & 0 & -Y_{45} & Y_5 + Y_{45} \end{bmatrix}$$

Plugging in the admittance values, the per-unit admittance matrix for the fundamental harmonic is

$$\mathbf{Y} = \begin{bmatrix} 1.6 - j7.2 & -0.96 + j4.3 & 0 & 0 & 0 \\ -0.96 + j4.3 & 2.3 - j8.1 & -1.3 + j3.8 & 0 & 0 \\ 0 & -1.3 + j3.8 & 42 - j28 & -41 + j24 & 0 \\ 0 & 0 & -41 + j24 & 59 - j35 & -18 + j10 \\ 0 & 0 & 0 & -18 + j10 & 18 - j10 \end{bmatrix}$$

There is only one current injected into a node in the circuit, and this is shown in the current matrix.

$$\mathbf{I} = \begin{bmatrix} 3.0 \\ 0 \\ 0 \\ 0 \\ 0 \end{bmatrix}$$

The matrix equation used to solve for node voltages is

$$\mathbf{V} = \mathbf{Y}^{-1}\mathbf{I}$$

Using this matrix equation, the node voltage column matrix was found to be

$$\mathbf{V} = \begin{bmatrix} 0.98 \\ 0.98 \\ 0.98 \\ 0.98 \\ 0.98 \\ \\ \end{bmatrix}$$

These node voltages were then used to calculate the fundamental harmonic of the current in each lumped load and home. For the lumped loads this current is given by

$$I_{Lm} = V_m \times Y_{Lm}$$

where *m* is the node number. Using this formula the lumped load currents were found to be

$$I_{L1} = 0.98 \times \ 0.035 - j0.020 \ = 0.039\, pu$$

$$I_{L2} = 0.98 \times \ 0.035 - j0.020 \ = 0.039\, pu$$

To find the currents at each home, first currents flowing through the equivalent node admittances were obtained. This is given by

$$I_m = V_m \times Y_m$$

Using this formula, the currents for nodes 3~5 were obtained.

$$I_3 = 0.98 \times \ 1.4 - j0.79 \ \times 10^{-4} \ = 1.6 \times 10^{-4}\, pu$$

$$I_4 = 0.98 \times \ 2.1 - j1.2 \ \times 10^{-4} \ = 2.3 \times 10^{-4}\, pu$$

$$I_5 = 0.98 \times \quad 1.4 - j0.79 \quad \times 10^{-4} \quad = 1.6 \times 10^{-4}\, pu$$

Since each home at a given node has the same admittance, the current at each home is divided evenly between each home connected to the same transformer. Let H_m, be the number of homes connected to the transformer at node *m*. The current for each home at node *m* is given by

$$I_{Hm} = \frac{I_m}{H_m}$$

Using this formula the home currents were calculated.

$$I_{H3} = \frac{1.6 \times 10^{-4}}{2} = 7.9 \times 10^{-5}\, pu$$

$$I_{H4} = \frac{2.3 \times 10^{-4}}{3} = 7.8 \times 10^{-5}\, pu$$

$$I_{H5} = \frac{1.6 \times 10^{-4}}{2} = 7.8 \times 10^{-5}\, pu$$

To check if this is a reasonable calculation the per-unit value was multiplied by the base current to obtain the actual RMS current to a home.

$$I'_{H3} = I_{H3} \times K_I = 7.8 \times 10^{-5} \times 300 \times 10^3 = 23\ A$$

This value is reasonable for an individual home since

$$P'_{H3} = V'_{H3} I'_{H3} \lambda_{H3} \approx 120 \times 23 \times 0.87 = 2.4\ kW$$

which is close to the given load active power of $2.5\ kW$.

5.6 Calculating Circuit Model Parameters for Harmonics

5.6.1 Circuit Model for Harmonics

For harmonic analysis new circuit model parameters must be calculated. Figure 5.6 shows the circuit model for loads for harmonic frequencies. In this figure, *R* and *X* are the resistance and reactance calculated for the fundamental, and *n* is the harmonic order. The current harmonics produced are modeled by a current source producing current J_n in parallel with the load impedance. All of the lumped loads and homes in the circuit are modeled in this way.

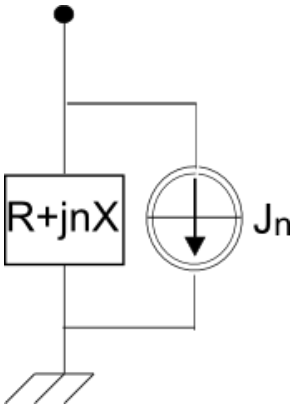

Figure 5.6 Load model for harmonics

The reactances of the distribution lines and transformers are also multiplied by the harmonic order, *n*. For example the reactance of the line between nodes 1 and 2 for the *n*-order harmonic is,

$$X_{12,n} = nX_{12}$$

where X_{12} is the reactance of the line for the fundamental. The RMS value of the *n*-order harmonic current produced by a load is given by

$$J_n = C\frac{I}{n^{\alpha}},$$

where *I* is the magnitude of the fundamental current, and *C* and α are constants that describe the distribution of current harmonics generated by each load. A typical value for α is

$$\alpha = 1.5$$

C can be calculated from the current harmonic distortion coefficient, δ_i of the load. For a given value of δ_i, the value of *C* is

$$C = \frac{\delta_i}{\sqrt{\sum_{n \in N_d} \frac{1}{n^{2\alpha}}}}$$

where N_d is the set of harmonics produced by the load. For most single-phase loads this set consists of all odd order harmonics. Harmonic analysis of this circuit was performed up to the 11^{th} harmonic using a computer model.

$$(3, 5, 7, 9, 11) \in N_d$$

To verify computer modeling, the circuit parameters were recalculated by hand for the third harmonic, and nodal analysis was performed to obtain the voltage RMS values for the third order harmonic.

The current distortion coefficient of each lumped load and home was assumed to be

$$\delta_i = 0.12$$

The value of *C* for each lumped load and home was calculated to be

$$C = \frac{0.12}{\sqrt{\frac{1}{3^3} + \frac{1}{5^3} + \frac{1}{7^3} + \frac{1}{9^3} + \frac{1}{11^3}}} = 0.54$$

5.6.2 Transformer Impedance Calculation for Harmonics

Let $\boldsymbol{Z}_{TM,n}$ be the impedance of the transformer at node M for the *n*-order harmonic, and let R_{TM} and X_{TM} be the resistance and reactance for the fundamental. The formula used to calculate the harmonic impedance is

$$\boldsymbol{Z}_{TM,n} = R_{TM} + jnX_{TM}$$

For the third harmonic, the transformer impedances are

$$\boldsymbol{Z}_{T1,3} = j3 \times 0.023 = j0.069\ pu$$

$$\boldsymbol{Z}_{T3,3} = 1.7 + j3 \times 17 = 1.7 + j51\ pu$$

$$\boldsymbol{Z}_{T4,3} = \boldsymbol{Z}_{T3,3} = 1.7 + j51\ pu$$

$$\boldsymbol{Z}_{T5,3} = 0.82 + j3 \times 8.2 = 0.82 + j25\ pu$$

5.6.2 Lumped Load Parameters Calculation for Harmonics

The lumped load impedances at node *m* were calculated using the expression

$$\boldsymbol{Z}_{Lm,n} = R_{Lm} + jnX_{Lm} = Re\ \frac{1}{\boldsymbol{Y}_{Lm}} + jn \times Im\ \frac{1}{\boldsymbol{Y}_{Lm}}$$

Plugging into the formula, impedance of the lumped load at node 1 for the third harmonic was obtained.

$$\boldsymbol{Z}_{L1,3} = Re\ \frac{1}{0.035 - j0.020} + j3 \times Im\ \frac{1}{0.035 - j0.020} = 22 + j37\ pu$$

$$\boldsymbol{Z}_{L2,3} = \boldsymbol{Z}_{L1,3} = 22 + j37\ pu$$

The current *n*-order harmonic produced by each lumped load is given by

$$J_{Lm,n} = C\frac{I_{Lm}}{n^{\alpha}}$$

For the third order harmonic, the currents produced by the lumped loads at nodes 1 and 2 are

$$J_{L1,3} = 0.54 \times \frac{0.040}{3^{1.5}} = 0.0041\ pu$$

$$J_{L2,3} = 0.54 \times \frac{0.039}{3^{1.5}} = 0.0040\ pu$$

5.6.3 Home Parameters for Harmonics

The home parameters for harmonics were calculated similar to the lumped load parameters. As previously mentioned, the home admittances are assumed to be all equal meaning the impedances are also the same. The formula used for calculation of the home impedance is

$$\boldsymbol{Z}_{H,n} = R_H + jnX_H = Re\ \frac{1}{\boldsymbol{Y}_H} + jn \times Im\ \frac{1}{\boldsymbol{Y}_H}$$

The home impedance for the third harmonic is

$$\boldsymbol{Z}_{H,3} = Re\ \frac{1}{6.9 - j3.9\ \times 10^{-5}} + j3 \times Im\ \frac{1}{6.9 - j3.9\ \times 10^{-5}} = 11000 + j19000\ pu$$

Each group of homes connected to the same transformer has the same fundamental current, so the current harmonics produced by each home in that group are the same. Let $J_{Hm,n}$ be the *n*-order current harmonic produced by a home connected to transformer *m*.

$$J_{Hm,n} = C\frac{I_{Hm}}{n^{\alpha}}$$

For the third order harmonic

$$J_{H3,3} = 0.54 \times \frac{7.8 \times 10^{-5}}{3^{1.5}} = 8.1 \times 10^{-6}\ pu$$

$$J_{H4,3} = 0.54 \times \frac{7.8 \times 10^{-5}}{3^{1.5}} = 8.0 \times 10^{-6}\ pu$$

$$J_{H5,3} = 0.54 \times \frac{7.8 \times 10^{-5}}{3^{1.5}} = 8.1 \times 10^{-6}\ pu$$

5.6.4 Distribution Line Impedances for Harmonics

Let $\boldsymbol{Z}_{ab,n}$ be the line impedance between nodes *a* and *b* for the *n*-order harmonic, and let $\boldsymbol{Z}_{ab}$ be the previously computed line impedance between the same two nodes for the fundamental. The harmonic impedance is calculated by

$$\boldsymbol{Z}_{ab,n} = Re\ \boldsymbol{Z}_{\boldsymbol{ab}}\ + jn \times Im\ \boldsymbol{Z}_{ab}\ = R_{ab} + jnX_{ab}$$

For the third harmonic the calculated line impedances are

$$\boldsymbol{Z}_{s,3} = 0.070 + j3 \times 0.31 = 0.070 + j0.93\ pu$$

$$\boldsymbol{Z}_{12,3} = 0.050 + j3 \times 0.22 = 0.050 + j0.67\ pu$$

$$\boldsymbol{Z}_{23,3} = 0.083 + j3 \times 0.24 = 0.083 + j0.71\ pu$$

$$\boldsymbol{Z}_{34,3} = 0.018 + j3 \times 0.011 = 0.018 + j0.032\ pu$$

$$\boldsymbol{Z}_{45,3} = 0.042 + j3 \times 0.025 = 0.042 + j0.074\ pu$$

5.7 Nodal Analysis for the Third Harmonic

5.7.1 Calculating Node Admittances and Currents

For node 1 the line impedance $\boldsymbol{Z}_{s,3}$ is in series with transformer impedance $\boldsymbol{Z}_{T1,3}$. These impedances were combined into an equivalent impedance.

$$\boldsymbol{Z}_{E1,3} = \boldsymbol{Z}_{s,3} + \boldsymbol{Z}_{T1,3} = 0.070 + j0.93 + j0.069 = 0.070 + j1.0\ pu$$

This impedance is in parallel with the lumped load impedance at node 1. Therefore they can be combined to form the node 1 admittance.

$$\boldsymbol{Y}_{1,3} = \frac{1}{\boldsymbol{Z}_{E1,3}} + \frac{1}{\boldsymbol{Z}_{L1,3}} = \frac{1}{0.070 + j1.0} + \frac{1}{22 + j37} = 0.082 - j1.0\ pu$$

The current injected into node 1 is

$$I_{1,3} = J_{L1,3} = 0.0041\ pu$$

The admittance at node 2 is equal to the lumped load admittance.

$$\boldsymbol{Y}_{2,3} = \frac{1}{\boldsymbol{Z}_{L2,3}} = \frac{1}{22 + j37} = 0.012 - j0.02\ pu$$

The current injected into node 2 is

$$I_{2,3} = J_{L2,3} = 0.0040\ pu$$

For nodes 3, 4, and 5, the home impedances and the harmonic current sources are all in parallel. Let the number of homes connected to transformer *m* be H_m. Since the home impedances are all the same, the equivalent home impedance is given by

$$\boldsymbol{Z}_{Em,3} = \frac{1}{H_m \times \frac{1}{\boldsymbol{Z}_{H,3}}}$$

The calculated equivalent impedances are

$$\boldsymbol{Z}_{E3,3} = \frac{1}{2 \times \frac{1}{11000 + j19000}} = 5500 + j9300\ pu$$

$$\boldsymbol{Z}_{E4,3} = \frac{1}{3 \times \frac{1}{11000 + j19000}} = 3600 + j6200\ pu$$

$$\boldsymbol{Z}_{E5,3} = \boldsymbol{Z}_{E3,3} = 5500 + j9300\ pu$$

The parallel current sources are also the same for every home connected to transformer *m*, and they can be combined into an equivalent current.

$$J_{Em,3} = H_m \times J_{Hm,3}$$

$$J_{H3,3} = 0.54 \times \frac{7.8 \times 10^{-5}}{3^{1.5}} = 8.1 \times 10^{-6}\ pu$$

$$J_{H4,3} = 0.54 \times \frac{7.8 \times 10^{-5}}{3^{1.5}} = 8.0 \times 10^{-6}\ pu$$

$$J_{H5,3} = 0.54 \times \frac{7.8 \times 10^{-5}}{3^{1.5}} = 8.1 \times 10^{-6}\ pu$$

The calculated equivalent currents are

$$J_{E3,3} = 2 \times 8.1 \times 10^{-6} = 1.6 \times 10^{-5}\ pu$$

$$J_{E4,3} = 3 \times 8.0 \times 10^{-6} = 2.4 \times 10^{-5}\ pu$$

$$J_{E5,3} = 2 \times 8.1 \times 10^{-6} = 1.6 \times 10^{-5}\ pu$$

The equivalent circuit of combined home loads connected to the transformer is shown in Figure 5.7.

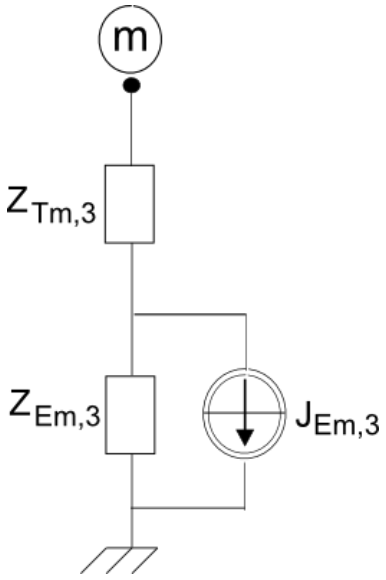

Figure 5.7 Equivalent circuit of combined home loads connected to transformer at node *m*

The Norton equivalent impedance of this circuit, which is the node impedance, is the series combination of the circuit impedances. For node *m*,

$$\boldsymbol{Z}_{m,3} = \boldsymbol{Z}_{Em,3} + \boldsymbol{Z}_{Tm,3.}$$

Then the node admittance is

$$\boldsymbol{Y}_{m,3} = \frac{1}{\boldsymbol{Z}_{m,3}} = \frac{1}{\boldsymbol{Z}_{Em,3} + \boldsymbol{Z}_{Tm,3}}$$

The calculated node admittances are

$$\boldsymbol{Y}_{3,3} = \frac{1}{5500 + j9300 + 1.7 + j51} = \ 4.7 - j8.0 \ \times 10^{-5}\, pu$$

$$\boldsymbol{Y}_{4,3} = \frac{1}{3600 + j6200 + 1.7 + j51} = \ 7.0 - j12 \ \times 10^{-5}\, pu$$

$$\boldsymbol{Y}_{5,3} = \frac{1}{5500 + j9300 + 0.82 + j25} = \ 4.7 - j8.0 \ \times 10^{-5}\, pu$$

The Norton equivalent current of the circuit in Figure 5.7, which is the node current is

$$I_{m,3} = J_{Em,3} \times \frac{\boldsymbol{Z}_{EqM,3}}{\boldsymbol{Z}_{EqM,3} + \boldsymbol{Z}_{TM,3}}$$

The calculated node currents for the third harmonic are

$$I_{3,3} = 1.6 \times 10^{-5} \times \frac{5500 + j9300}{5500 + j9300 + 1.7 + j51} = 1.6 \times 10^{-5}\, pu$$

$$I_{4,3} = 2.4 \times 10^{-5} \times \frac{3600 + j6200}{3600 + j6200 + 1.7 + j51} = 2.4 \times 10^{-5}\, pu$$

$$I_{5,3} = 1.6 \times 10^{-5} \times \frac{5500 + j9300}{5500 + j9300 + 0.82 + j25} = 1.6 \times 10^{-5}\, pu$$

5.7.2 Calculating Line Admittances

The line admittances are given by

$$\boldsymbol{Y}_{ab,3} = \frac{1}{\boldsymbol{Z}_{ab,3}}$$

The calculated line admittances are

$$\boldsymbol{Y}_{12,3} = \frac{1}{0.05 + j0.67} = 0.11 - j1.5\ pu$$

$$\boldsymbol{Y}_{23,3} = \frac{1}{0.083 + j0.71} = 0.16 - j1.4\ pu$$

$$\boldsymbol{Y}_{34,3} = \frac{1}{0.018 + j0.032} = 13 - j24\ pu$$

$$\boldsymbol{Y}_{45,3} = \frac{1}{0.042 + j0.074} = 5.8 - j10\ pu$$

5.7.4 Using Admittance Matrix for Nodal Analysis of Third Harmonic

Once all elements were combined into admittances and current sources, the admittance matrix was made. The admittance matrix for the third harmonic

$$\mathbf{Y}_3 = \begin{bmatrix} Y_{1,3} + Y_{12,3} & -Y_{12,3} & 0 & 0 & 0 \\ -Y_{12,3} & Y_{2,3} + Y_{12,3} + Y_{23,3} & -Y_{23,3} & 0 & 0 \\ 0 & -Y_{23,3} & Y_{3,3} + Y_{23,3} + Y_{34,3} & -Y_{34,3} & 0 \\ 0 & 0 & -Y_{34,3} & Y_{4,3} + Y_{34,3} + Y_{45,3} & -Y_{45,3} \\ 0 & 0 & 0 & -Y_{45,3} & Y_{5,3} + Y_{45,3} \end{bmatrix}$$

The admittance matrix with all data filled in is

$$\mathbf{Y}_3 = \begin{bmatrix} 0.20 - j2.5 & -0.11 + j1.5 & 0 & 0 & 0 \\ -0.11 + j1.5 & 0.29 - j2.9 & -0.16 + j1.4 & 0 & 0 \\ 0 & -0.16 + j1.4 & 14 - j25 & -13 + j24 & 0 \\ 0 & 0 & -13 + j24 & 19 - j34 & -5.8 + j10 \\ 0 & 0 & 0 & -5.8 + j10 & 5.8 - j10 \end{bmatrix}$$

The current column matrix consists of all the calculated node currents.

$$\mathbf{I}_3 = \begin{bmatrix} I_{1,3} \\ I_{2,3} \\ I_{3,3} \\ I_{4,3} \\ I_{5,3} \end{bmatrix}$$

The current matrix with all data filled in is

$$\mathbf{I}_3 = \begin{bmatrix} 0.0041 \\ 0.0040 \\ 1.6 \times 10^{-5} \\ 2.4 \times 10^{-5} \\ 1.6 \times 10^{-5} \end{bmatrix}$$

The matrix equation is

$$\mathbf{V}_3 = \mathbf{Y}_3^{-1}\mathbf{I}_3$$

Solving for the node voltages

$$\mathbf{V}_3 = \begin{bmatrix} 0.0076 \\ 0.01 \\ 0.0099 \\ 0.0099 \\ 0.0099 \\ \\ \end{bmatrix}$$

5.8 Computer Modeling of Distribution System

5.8.1 Computer Modeling for Normal Loads

A distribution system modeling program was written in Matlab to perform nodal analysis for any number of odd-order harmonics. The Matlab code for this program is provided in Appendix A. In the program fewer approximations were made than in the hand calculations described in the previous sections. The program calculates the CRMS values of voltage harmonics, RMS values of voltages, and the total harmonic distortion for every node. The formula used for RMS value of voltage for node M in this program is

$$\left\| V_m \right\| = \sqrt{\sum_{n \in N} V_{m,n}^{\ 2}}$$

where *N* is the set of all harmonics in the system including the fundamental.

The formula used for voltage total harmonic distortion at node *m* is

$$\delta_{vm} = \frac{\sqrt{\sum_{n \in N_d} V_{m,n}^{\ 2}}}{V_{m,1}} \times 100\%$$

where N_d is the set of harmonics in the system excluding the fundamental. The results of running the program with the same parameters used for the previous hand calculations are shown in Figure 5.8. Observe that the system is operating under normal conditions. The node voltages are all very close to the base values, and voltage distortion is well within acceptable limits.

```
NODE RMS VOLTAGES [V]
V1 = 7820.8
V2 = 7771.2
V3 = 7770.4
V4 = 7770.3
V5 = 7770.3

TOTAL HARMONIC DISTORTION
Node 1 THD = 1.30 %
Node 2 THD = 1.75 %
Node 3 THD = 1.76 %
Node 4 THD = 1.76 %
Node 5 THD = 1.76 %

CRMS VOLTAGE HARMONICS [V]
n = 3:
V1  =  63.2,  V2  =  84.4,  V3  =  84.7,  V4  =  84.7,  V5  =  84.7,

n = 5:
V1  =  48.5,  V2  =  64.8,  V3  =  65.0,  V4  =  65.0,  V5  =  65.0,

n = 7:
V1  =  40.8,  V2  =  54.6,  V3  =  54.7,  V4  =  54.8,  V5  =  54.8,

n = 9:
V1  =  36.0,  V2  =  48.0,  V3  =  48.2,  V4  =  48.2,  V5  =  48.2,

n = 11:
V1  =  32.5,  V2  =  43.4,  V3  =  43.6,  V4  =  43.6,  V5  =  43.6,
```

Figure 5.8 Results of computer modeling with typical loads

5.8.2 Verification of Results

To verify that the results from the program are valid, the node values for the fundamental and third harmonic will be compared with the previously explained hand calculations. By multiplying the base voltage by the per-unit node voltage column matrices (one for the fundamental, the other for the third harmonic), the column matrices of actual node voltages are obtained.

$$\mathbf{V}'_1 = K_V \times \mathbf{V}_1 = 7970 \times \begin{bmatrix} 0.98 \\ 0.98 \\ 0.98 \\ 0.98 \\ 0.98 \\ \\ \end{bmatrix} = \begin{bmatrix} 7800 \\ 7800 \\ 7800 \\ 7800 \\ 7800 \\ \\ \end{bmatrix} \text{ V}$$

$$\mathbf{V}'_3 = K_V \times \mathbf{V}_3 = 7970 \times \begin{bmatrix} 0.0076 \\ 0.01 \\ 0.0099 \\ 0.0099 \\ 0.0099 \\ \\ \end{bmatrix} = \begin{bmatrix} 61 \\ 80 \\ 79 \\ 79 \\ 79 \\ \\ \end{bmatrix} \text{ V}$$

Comparing the computer modeling results with the hand calculations, it is observed that the difference is small. The fundamental the voltages calculated by hand were about 20 V higher than the computer results. This is less than one percent difference. For the third harmonic, the largest difference was about 5 V out of 79 V, which is about 6%. Since the hand calculation used more rounding and approximations, this error is reasonable. With this comparison it is demonstrated that the results of the modeling program seem to be correct.

5.8.3 Computer Modeling for Loads with EVs

Once the distribution system modeling program was verified, the modeling program was run again with parameters representing EV loads. A worst case study was done to examine the most detrimental effects possible. The current distortion coefficient of the battery chargers was assumed to be 0.2, which is the worst case since standards limit manufacturers from selling EV chargers with higher than 0.2 distortion coefficient [40]. The distortion coefficients of EV chargers and of the power system loads are assumed to be mutually random and thus, orthogonal. With this assumption, the new distortion coefficient of the combined loads of EV chargers and previously modeled loads is

$$\delta_i' = \sqrt{\delta_{i,EV}{}^2 + \delta_i^2} = \sqrt{0.2^2 + 0.12^2} = 0.22$$

The EV was modeled as an additional 3.5 kW load on top of the normal home loads for a total of 6 kW per home. Lumped load 1 had a total of 451 customers. If every customer had an EV,

$$P_{EV1} = 451 \times 3.5 = 1.6\ MW.$$

Lumped load 2 had 379 customers. If all of them had an EV, then

$$P_{EV2} = 379 \times 3.5 = 1.3\ MW.$$

Since EV chargers are required to have a power factor no less than 0.95, this model uses 0.95 as the EV power factor.

$$\lambda_{EV} = 0.95$$

so

$$S_{EV1} = \frac{P_{EV1}}{\lambda_{EV}} = \frac{1.6}{0.95} = 1.7\ MVA$$

$$S_{EV2} = \frac{P_{EV2}}{\lambda_{EV}} = \frac{1.3}{0.95} = 1.4\ MVA$$

These will be added to the normal apparent power which was used to model the circuit previously.

These chosen parameters are the worst-case scenario, with 100% EV penetration, all charging at the same time, highest current distortion coefficient permissible, and lowest permissible power factor. The results of computer modeling of this scenario are shown in Figure 5.9.

```
NODE RMS VOLTAGES [V]
V1 = 7674.7
V2 = 7584.6
V3 = 7582.8
V4 = 7582.6
V5 = 7582.5

TOTAL HARMONIC DISTORTION
Node 1 THD = 4.64 %
Node 2 THD = 6.19 %
Node 3 THD = 6.22 %
Node 4 THD = 6.22 %
Node 5 THD = 6.22 %

CRMS VOLTAGE HARMONICS [V]
n = 3:
V1  = 221.9,  V2  = 292.5,  V3  = 293.7,  V4  = 293.7,  V5  = 293.8,

n = 5:
V1  = 169.1,  V2  = 222.7,  V3  = 223.7,  V4  = 223.7,  V5  = 223.7,

n = 7:
V1  = 142.2,  V2  = 187.2,  V3  = 188.0,  V4  = 188.0,  V5  = 188.0,

n = 9:
V1  = 125.1,  V2  = 164.7,  V3  = 165.4,  V4  = 165.4,  V5  = 165.4,

n = 11:
V1  = 113.0,  V2  = 148.8,  V3  = 149.4,  V4  = 149.4,  V5  = 149.4,
```

Figure 5.9 Computer model results for worst case scenario

5.8.4 Interpretation of Results

This worst case scenario shows very important information. The lowest voltage is 7582.5 V at node 5. The per-unit value of this is

$$V_5 = \frac{7582.5}{7970} = 0.95$$

Standards require that power utilities keep all system voltages at 0.95 or higher, so this node voltage exactly meets this standard. This means if there was 100% EV penetration in this system, all with the worst load quality allowable and charging at the same time, voltage profile would not be a problem. On the other hand, voltage distortion would be a problem. Nodes 2~4 all have voltage total harmonic distortion around 6%, which is slightly greater than the maximum allowable limit of 5%.

Modeling was repeated for different penetration levels until the voltage distortion level reached about 5%. This penetration level was found to be 60%, which is still an unlikely number for the near future. It should also be noted that measurements from the Transit Connect Electric battery charging cycle indicate that some EVs have extremely good load quality. If most of the EV charger loads are similar to the Transit Connect, then no harmonic problems could be expected, and as previously mentioned, voltage profile would also not be a problem even with 100% penetration.

CHAPTER 6. CONCLUSION

6.1 Conclusion

This research focused on the present state of electric vehicles in the market and the effects that these vehicles could have on residential distribution systems. The results of the investigation into the EV market are that currently only 0.01% of vehicles in the U.S. are EVs, and there are many disadvantages of EVs to consumers which are keeping EVs from gaining the same level of market penetration as their competitors. The most significant disadvantages are high cost, limited driving range on battery, and long battery charging time. Government incentives have helped to make EVs more affordable, but these incentives are not permanent. Rather they are only designed to promote the early advancement of EVs with the assumption that their cost will decrease in the near future, but there are some economic and political forces that may prevent the cost from decreasing. China's monopoly on rare earth minerals is an issue of particular concern.

In terms of energy efficiency, EVs are advantageous. In a rough calculation of the efficiencies of energy delivery processes of EVs and GVs, it was found that energy savings by EVs could be around 25%. Although the efficiency calculations were not very accurate, they demonstrate that it is very likely that EVs use less energy than GVs. EVs could also significantly reduce carbon emissions and the rate of depletion of fossil fuels, but to maximize this benefit a greater percentage of nuclear or renewable resource energy generation should be used.

In measurements of an actual EV battery charging cycle, it was discovered that some EV battery chargers have excellent load properties. The power factor was near unity and current

harmonic distortion was less than 5%. These measured values exceed the standards of less than 20% harmonic distortion and greater than 0.95 power factor.

Modeling of a residential power system showed that it is unlikely that EVs will cause significant power system problems in the near future. Real power system data was used in the calculation of the circuit model, and a computer model was programmed in Matlab to perform nodal analysis for harmonics. In the end, even assuming 100% penetration of EVs in this neighborhood with all charging at once, it is unlikely that there will be any detrimental effects. It is possible that this is not true for other residential systems, but with current EV penetration levels problems are unlikely.

REFERENCES

[1] M. Bellis, "History of Electric Vehicles The Early Years, Electric Cars from 1830 to 1930," [Online]. Available: http://inventors.about.com/od/estartinventions/a/History-Of-Electric-Vehicles.htm. [Accessed 9 May 2012].

[2] History.com, "The end of the road for Oldsmobile," 29 April 2012. [Online]. Available: http://www.history.com/this-day-in-history/the-end-of-the-road-for-oldsmobile. [Accessed 9 May 2012].

[3] Ford Motor Company, "Model T Facts," [Online]. Available: http://media.ford.com/article_display.cfm?article_id=858. [Accessed 9 May 2012].

[4] History.com, "Model T," 2012. [Online]. Available: http://www.history.com/topics/model-t. [Accessed 9 May 2012].

[5] "Why Electric Cars?," [Online]. Available: http://www.whokilledtheelectriccar.com/why. [Accessed 9 May 2012].

[6] J. Voelcker, "Electric Car Sales for 2011: Modest First Year Numbers Hardly a Surprise," 4 January 2012. [Online]. Available: http://www.greencarreports.com/news/1071246_electric-car-sales-for-2011-modest-first-year-numbers-hardly-a-surprise. [Accessed 9 May 2012].

[7] WardsAuto Group, "U.S. Car and Truck Sales, 1931-2011," [Online]. Available: http://wardsauto.com/keydata/historical/UsaSa01summary. [Accessed 9 May 2012].

[8] "Qualified Plug-in Electric Vehicle Credit," 29 June 2009. [Online]. Available: http://www.irs.gov/irb/2009-26_IRB/ar07.html. [Accessed 9 May 2012].

[9] Green Car Journal Editors, "California Under Pressure, Modifies 1998 ZEV Mandate," 13 January 2008. [Online]. Available: http://www.greencar.com/articles/california-under-pressure-modifies-1998-zev-mandate.php. [Accessed 9 May 2012].

[10] WIRED, "California Cuts ZEV Mandate In Favor of Plug-In Hybrids," 27 March 2008. [Online]. Available: http://www.wired.com/autopia/2008/03/the-california/. [Accessed 9 May 2012].

[11] C. Squatriglia, "Better Place Unveils an Electric Car Battery Swap Station," 13 May 2009. [Online]. Available: http://www.wired.com/autopia/2009/05/better-place/. [Accessed 9 May 2012].

[12] J. Doom, "Battery Prices For Electric Vehicles Fall 14%, BNEF Says," Bloomberg, 16 April 2012. [Online]. Available: http://www.bloomberg.com/news/2012-04-16/battery-prices-for-electric-vehicles-fall-14-bnef-says.html. [Accessed 20 May 2012].

[13] Nissan USA, "Answers: Charging," [Online]. Available: http://www.nissanusa.com/leaf-

electric-car/index?dcp=ppn.63023882.&dcc=0.240189300#/leaf-electric-car/faq/list/charging. [Accessed 9 May 2012].

[14] A. Giddens and M. Alice, "Guest Commentary: The economy might be growing, but it's not greening," The Denver Post, 16 May 2011. [Online]. Available: http://www.denverpost.com/opinion/ci_18011019Guest. [Accessed 20 May 2012].

[15] P. Valdez-Dapena, "GM stops Volt production for 5 weeks," 2 March 2012. [Online]. Available: http://money.cnn.com/2012/03/02/autos/volt_production_stopped/index.htm?iid=EL. [Accessed 9 May 2012].

[16] C. Demorro, "Nissan Leaf, Chevy Volt Fall Short Of 2011 Sales Goals, But That's OK," 5 January 2012. [Online]. Available: http://gas2.org/2012/01/05/nissan-leaf-chevy-volt-fall-short-of-2011-sales-goals-but-that%E2%80%99s-ok/. [Accessed 9 May 2012].

[17] D. Walsh, "Amid all its troubles, A123 Systems gets extension on Energy Department loan," 12 April 2012. [Online]. Available: http://www.crainsdetroit.com/article/20120412/FREE/120419955#. [Accessed 9 May 2012].

[18] U.S. Department of Energy, "Alternative Fuels and Advanced Vehicles Data Center: All Incentives and Laws Sorted by Incentive," 15 June 2011. [Online]. Available: http://www.afdc.energy.gov/afdc/laws/matrix/incentive. [Accessed 20 May 2012].

[19] E. Strickland, "Complaints Over China's Rare Earth Export Policies Get Serious," IEEE Spectrum, 13 March 2012. [Online]. Available: http://spectrum.ieee.org/tech-talk/semiconductors/materials/complaints-over-chinas-rare-earth-export-policies-get-serious. [Accessed 20 May 2012].

[20] K. Bourzac, "Can the U.S. Rare-Earth Industry Rebound?," Technology Review, 29 October 2010. [Online]. Available: http://www.technologyreview.com/energy/26655/?p1=MstCom. [Accessed 20 May 2012].

[21] U.S. Energy Information Administration, "Electric Power Annual - Summary Statistics for the United States," 9 November 2011. [Online]. Available: http://205.254.135.7/electricity/annual/html/tablees1.cfm. [Accessed 20 May 2012].

[22] Electropaedia, "Electricity Generation Using Steam Turbines," 2005. [Online]. Available: http://www.mpoweruk.com/steam_turbines.htm. [Accessed 22 May 2012].

[23] Turbines Info, "Steam Turbine Efficiency," 7 August 2011. [Online]. Available: http://www.turbinesinfo.com/steam-turbine-efficiency/. [Accessed 22 May 2012].

[24] C. Johnson, "Automotive Engine," February 2003. [Online]. Available: http://mb-soft.com/public2/engine.html. [Accessed 22 May 2012].

[25] "Improving IC Engine Efficiency," University of Washington, [Online]. Available: http://courses.washington.edu/me341/oct22v2.htm. [Accessed 22 May 2012].

[26] International Electrotechnical Commission, "Efficient Electrical Energy Transmission and Distribution," 2007. [Online]. Available: http://www.iec.ch/about/brochures/pdf/technology/transmission.pdf. [Accessed 20 May 2012].

[27] Mitsubishi Motors, "Compare ES & SE Trim Specs," 2012. [Online]. Available: http://i.mitsubishicars.com/miev/features/compare. [Accessed 20 May 2012].

[28] Nissan USA, "Nissan LEAF Features and Specifications," [Online]. Available: http://www.nissanusa.com/leaf-electric-car/specs-features/index#/leaf-electric-car/specs-features/index. [Accessed 20 May 2012].

[29] Tesla Motors, "Roadster Features and Specifications," [Online]. Available: http://www.teslamotors.com/roadster/specs. [Accessed 20 May 2012].

[30] Azure Dynamics, "Transit Connect Electric Specifications & Ordering Guide," April 2011. [Online]. Available: http://www.azuredynamics.com/products/documents/SPC501074-A_TCE_Specifications_and_Ordering_Guide.pdf. [Accessed 20 May 2012].

[31] "Tesla Polyphase Induction Motors," All About Circuits, [Online]. Available: http://www.allaboutcircuits.com/vol_2/chpt_13/7.html. [Accessed 20 May 2012].

[32] ABB, "DriveIT Permanent Magnet Motors," March 2004. [Online]. Available: http://www05.abb.com/global/scot/scot234.nsf/veritydisplay/b126d92180c4791dc125784f0037f9cb/$file/permanent%20magnet%20motors%20gb%2005-2004.pdf. [Accessed 20 May 2012].

[33] J. Amirault, J. Chien, S. Garg, D. Gibbons, B. Ross, M. Tang, J. Xing, I. Sidhu, P. Kaminsky and B. Tenderich, "The Electric Vehicle Battery Landscape: Opportunities and Challenges," 21 December 2009. [Online]. Available: http://cet.berkeley.edu/dl/BatteryBrief_final.pdf. [Accessed 20 May 2012].

[34] D. Andrea, Battery Management Systems for Large Lithium-Ion Battery Packs, Norwood, MA: Artech House, 2010.

[35] A. Virtanen, H. Haapala, S. Hännikäinen, T. Muhonen and H. Tuusa, "Calorimetric efficiency measurement of supercapacitors and lithium-ion batteries," in *Applied Power Electronics Conference and Exposition (APEC), 2011 Twenty-Sixth Annual IEEE*, 2011.

[36] Y. Hsien and C. Huang, "Li-ion battery charger based on digitally controlled phase-shifted full-bridge converter," *IET on Power Electronics,* vol. 4, no. 2, pp. 242-247, 2011.

[37] J. Wu, "Three-leg power converter topology for a battery charger," *IET on Power*

Electronics, vol. 4, no. 5, pp. 541-547, 2010.

[38] Y. Lu, K. Cheng and S. Zhao, "Power battery charger for electric vehicles," *Power Electronics, IET,* vol. 4, no. 5, pp. 580-586, 2011.

[39] Z. Fedyczak, Interviewee, *prof. of power electronics, Zielona Gora Univ. of Technology, Poland.* [Interview]. 2011.

[40] C. J. Gómez and M. M. Morcos, "Impact of EV Battery Chargers on the Power Quality of Distribution Systems," *IEEE Transactions on Power Delivery,* vol. 18, 2003.

[41] United States Census Bureau, "New Residential Sales Historical Data," 20 December 2011. [Online]. Available: http://www.census.gov/construction/nrs/historical_data/. [Accessed 9 May 2012].

[42] West Bank Living, "English Turn, New Orleans LA | February 2010 Home Sales and Real Estate Market Statistics," 26 March 2010. [Online]. Available: http://westbankliving.com/market-updates/english-turn-new-orleans-la-february-2010-home-sales-and-real-estate-market-statistics/. [Accessed 9 May 2012].

[43] Mitsubishi Motors Corporation, "Frequently Asked Questions," 2012. [Online]. Available: http://i.mitsubishicars.com/faq/battery. [Accessed 9 May 2012].

APPENDIX: MATLAB CODE FOR DISTRIBUTION SYSTEM MODEL

```
j=sqrt(-1);

%%%%%%%%%%%%%%%%%%%%%% Distribution System Data %%%%%%%%%%%%%%%%%%%%%%%%%

M=5; %M is the number of nodes.
H=3; %H is the number of nodes with a residential home transformer.
h=3; %H is the max number of homes on a single transformer.
N=11; %N is the highest order harmonic.
PL=1;
%Home transformers ratings
Home_Trans_S=[50 50 100]; %KVA ratings
Home_Trans_Rated_Zpu=[0.023 0.023 0.023]; %Rated per unit impedance
Home_Trans_XtoR=[10 10 10]; %X to R ratios IEEE Std C37.010-1999

%Substation transformer ratings
Subs_Trans_Rated_Zpu=0.023;
Subs_Trans_XtoR=28;
Subs_Trans_S=36; %Apparent power rating in MVA

%Lumped loads parameters
Lumped_Load_S=[(8.965-4.642)/3+PL*1.662 (4.647/3-0.096)+PL*1.397]; %apparent power of
load in MVA
Lumped_Load_pf=[0.87 0.87];
Lumped_Load_dist=[0.13 0.13]; %current distortion coefficients
Lumped_Load_a=[1.5 1.5]; %alpha - the constant of harmonic exponential decrease

%Home loads parameters
Home_P=PL*[6  6  0   ; %active power in kW
        6  6  6 ;
        6  6  0   ];

Home_pf=[0.87  0.87  0     ;
         0.87  0.87  0.87  ;
         0.87  0.87  0     ];

Home_dist=[0.13  0.13  0; %current distortion coefficients
           0.13  0.13  0.13;
           0.13  0.13  0];

Home_a=[1.5 1.5 0; %alpha - the constant of harmonic exponential decrease
        1.5 1.5 1.5;
        1.5 1.5 0];

%Distribution lines parameters

Subs_Line_RL1=0.126;
Subs_Line_XL1=0.557;

RL1=zeros(M,M); %Line resistance between nodes for 60 Hz in ohms
RL1(1,2)= 0.0901;
RL1(2,3)= 0.149;
RL1(3,4)= 0.0326;
RL1(4,5)= 0.0754;

XL1=zeros(M,M); %Line inductance between nodes for 60 Hz in ohms
XL1(1,2)= 0.4020;
```

```
XL1(2,3)= 0.427;
XL1(3,4)= 0.0192;
XL1(4,5)= 0.0444;


%%%%%%%%%%%%%%%%%%%%%%%%%%% Per Unit Conversion %%%%%%%%%%%%%%%%%%%%%%%%%%%


%Single-Phase Per-Unit Bases for Sections a, b, and c
S_base=Subs_Trans_S*10^6;
Va_base=230*10^3/sqrt(3);
Vb_base=13.8*10^3/sqrt(3);
Vc_base=120;
Za_base=Va_base^2/S_base;
Zb_base=Vb_base^2/S_base;
Zc_base=Vc_base^2/S_base;
Ia_base=S_base/Va_base;
Ib_base=S_base/Vb_base;
Ic_base=S_base/Vc_base;

%Recalculate home transformers per unit impedance ratings to new S_base
Home_Trans_Zpu_Recalc=(Home_Trans_Rated_Zpu./(Home_Trans_S*1000))*S_base;

%Convert line parameters to per unit
Subs_Line_RL1pu=Subs_Line_RL1/Zb_base;
Subs_Line_XL1pu=Subs_Line_XL1/Zb_base;

RL1pu=RL1/Zb_base;
XL1pu=XL1/Zb_base;

%Convert lumped load parameters to per unit
Lumped_Load_Spu=Lumped_Load_S*10^6/S_base;

%Convert home load active power to per unit
Home_Ppu=Home_P*1000/S_base;


%%%%%%%%%%%%%%%%% Nodes 1 and 2 Modeling for Fundamental %%%%%%%%%%%%%%%%%

%Lumped Loads Admittance and Impedance Calculation
Lumped_Load_Ppu=Lumped_Load_Spu.*Lumped_Load_pf;
Lumped_Load_G1pu=Lumped_Load_Ppu/1^2;
Lumped_Load_Qpu=Lumped_Load_Spu.*sin(acos(Lumped_Load_pf));
Lumped_Load_B1pu=-Lumped_Load_Qpu/1^2;
Lumped_Load_Y1pu=Lumped_Load_G1pu+j*Lumped_Load_B1pu;
Lumped_Load_R1pu=real(1./Lumped_Load_Y1pu);
Lumped_Load_X1pu=imag(1./Lumped_Load_Y1pu);

%Calculate Substation Transformer Resistance and Reactance
Subs_Trans_R1pu=Subs_Trans_Rated_Zpu/sqrt(1+Subs_Trans_XtoR^2);
Subs_Trans_X1pu=Subs_Trans_R1pu*Subs_Trans_XtoR;
Subs_Trans_Z1pu=Subs_Trans_R1pu+j*Subs_Trans_X1pu;

%Calculate Substation Transformer to Node 1 Line Impedance
Subs_Line_Z1pu=Subs_Line_RL1pu+j*Subs_Line_XL1pu;

%Node 1 Norton Equivalent
Node_I1pu(M)=0;
```

```
Node_I1pu(1)=abs(1/(Subs_Trans_Z1pu+Subs_Line_Z1pu));%assume V1=1 pu
Node_Y1pu(1)=1/(Subs_Trans_Z1pu+Subs_Line_Z1pu)+Lumped_Load_Y1pu(1);

%Node 2 Norton Equivalent
Node_Y1pu(2)= Lumped_Load_Y1pu(2);


%%%%%%%%%%%%%%%%%%%% Nodes 3~4 Modeling for Fundamental %%%%%%%%%%%%%%%%%%%%

%Home Transformers Modeling
Home_Trans_R1pu=Home_Trans_Zpu_Recalc./((1+Home_Trans_XtoR.^2).^0.5);
Home_Trans_X1pu=Home_Trans_XtoR.*Home_Trans_R1pu;
Home_Trans_Z1pu=Home_Trans_R1pu+j*Home_Trans_X1pu;

%Home Loads Modeling
Home_G1pu=Home_Ppu./1^2;
Home_phi=acos(Home_pf);
Home_Q1pu=Home_Ppu.*(tan(Home_phi));
Home_B1pu=-Home_Q1pu./1^2;
Home_Y1pu=Home_G1pu+j*Home_B1pu;

Home_Z1pu=zeros(H,h);

for a=1:1:H
    for b=1:1:h
        if Home_Y1pu(a,b)~=0;
           Home_Z1pu(a,b)=1/Home_Y1pu(a,b);
        end
    end
end

Home_R1pu=real(Home_Z1pu);
Home_X1pu=imag(Home_Z1pu);

%Add parallel admittances at each node to obtain combined equivalent of
%home loads connected to transformer secondary
Equiv_Y1pu=sum(Home_Y1pu, 2).';
Equiv_Z1pu=1./Equiv_Y1pu;

%Find Norton equivalent admittance of each node to ground.
Home_Node_Z1pu=Equiv_Z1pu+Home_Trans_Z1pu;
Node_Y1pu=[Node_Y1pu 1./Home_Node_Z1pu];


%%%%%%%%%%%%%%%%%%%%%%% Distribution Lines Modeling %%%%%%%%%%%%%%%%%%%%%%%

ZL1pu=RL1pu+j*XL1pu;

%create YL - a matrix of the line admittances
YL1pu = zeros(M,M);
for a=1:1:M
    for b=1:1:M
        if ZL1pu(a,b) ~= 0,
           YL1pu(a,b) = 1/ZL1pu(a,b);
        end
    end
end
```

```
    %Use symmetry to fill in the remaining line impedances.
    %ie. YL12 = YL21.
    YL1pu=YL1pu+YL1pu.';


%%%%%%%%%%%%%%%%%%%%% Nodal Analysis for Fundamental %%%%%%%%%%%%%%%%%%%%%

%Non-diagonals of system admittance matrix are negative.
Y1pu = -YL1pu;

%Diagonal values are initalized to the node admittances.
for a=1:1:M
    Y1pu(a,a)=Node_Y1pu(a);
end

%Node to ground admittance is then added to the sum of the line admittances
%for that node.
for a=1:1:M
    for b=1:1:M
        if a ~= b, Y1pu(a,a) = Y1pu(a,a)+ YL1pu(a,b);
        end
    end
end

Z1pu=inv(Y1pu);

%Solve for Node voltages
Node_V1pu=abs(Z1pu*(Node_I1pu).').';
Node_V1=Node_V1pu*Vb_base;

%Solve for Home Fundamental Currents
Node_Sec_Vpu(H)=0;
Home_I1pu(H,h)=0;
Home_I1(H,h)=0;

for a=1:1:H
    Node_Sec_Vpu(a)=abs(Node_V1pu(a+2)*Equiv_Z1pu(a)/(Equiv_Z1pu(a)+
Home_Trans_Z1pu(a)));
    for b=1:1:h
        Home_I1pu(a,b)=abs(Node_Sec_Vpu(a)*Home_Y1pu(a,b));
        Home_I1(a,b)=Home_I1pu(a,b)*Ic_base;
    end
end

%Solve for lumped load fundamental currents
Lumped_Load_I1pu(1)=abs(Node_V1pu(1)*Lumped_Load_Y1pu(1));
Lumped_Load_I1pu(2)=abs(Node_V1pu(2)*Lumped_Load_Y1pu(2));
Lumped_Load_I1=Lumped_Load_I1pu*Ib_base;



%%%%%%%%%%%%%%%%%%%%% Nodal Analysis for Harmonics %%%%%%%%%%%%%%%%%%%%%%%

%Calculate C for each home
 den(H,h)=0;
 for a=1:1:H
     for b=1:1:h
```

```
        for n=3:2:N
                den(a,b)=den(a,b)+1/n^(2*Home_a(a,b));
        end
        den(a,b)=sqrt(den(a,b));
    end
 end
 Home_C=Home_dist./den;

 %Calculate C for Lumped Loads at nodes 1 and 2
 clear den
 den(2)=0;
for a=1:1:2
   for n=3:2:N
       den(a)=den(a)+1/n^(2*Lumped_Load_a(a));
   end
end
 den=den.^0.5;
 Lumped_Load_C=Lumped_Load_dist./den;


%Calculate Norton Equivalent for each node for n-order harmonic
Node_Vnpu(M)=0;
Node_Vpu=Node_V1pu;
Node_V=Node_V1;
Node_Vn=0;
 for n=3:2:N
     %Nodes 3~5
     clear Home_Jnpu;
     clear Equiv_Ynpu;
     clear Equiv_Jnpu;
     clear Home_Node_Inpu;
     Equiv_Ynpu(H)=0;
     Equiv_Jnpu(H)=0;
     Home_Ynpu=zeros(H,h);
     Home_Node_Inpu(H)=0;

        Home_Jnpu=Home_C.*Home_I1pu./(n.^Home_a);
        for a=1:1:H
            for b=1:1:h
                if Home_R1pu(a,b)+j*n*Home_X1pu(a,b)~=0
                   Home_Ynpu(a,b)=1/(Home_R1pu(a,b)+j*n*Home_X1pu(a,b));
                end
            end
        end

        for a=1:1:H
            for b=1:1:h
                Equiv_Ynpu(a)=Equiv_Ynpu(a)+Home_Ynpu(a,b);
                Equiv_Jnpu(a)=Equiv_Jnpu(a)+Home_Jnpu(a,b);
            end
            Equiv_Znpu(a)=1/Equiv_Ynpu(a);
            Trans_Znpu(a)=Home_Trans_R1pu(a)+j*n*Home_Trans_X1pu(a);
            Node_Znpu(a)=Equiv_Znpu(a)+Trans_Znpu(a);
            Home_Node_Ynpu(a)=1/Node_Znpu(a);

Home_Node_Inpu(a)=Equiv_Jnpu(a)*abs(Equiv_Znpu(a)/(Equiv_Znpu(a)+Trans_Znpu(a)));
         end
```

```
     %Nodes 1 and 2 Norton Equivalents
     Node2_Ynpu=1/(Lumped_Load_R1pu(2)+j*n*Lumped_Load_X1pu(2));
     Node2_Inpu=Lumped_Load_C(2)*Lumped_Load_I1pu(2)/n^Lumped_Load_a(2);
     Node1_Inpu=Lumped_Load_C(1)*Lumped_Load_I1pu(1)/n^Lumped_Load_a(1);

Node1_Subs_Znpu=Subs_Trans_R1pu+j*n*Subs_Trans_X1pu+real(Subs_Line_Z1pu)+j*n*imag(Subs
_Line_Z1pu);
     Node1_Ynpu=1/Node1_Subs_Znpu+1/(Lumped_Load_R1pu(1)+j*n*Lumped_Load_X1pu(1));
     Node_Ynpu=[Node1_Ynpu Node2_Ynpu Home_Node_Ynpu];
     Node_Inpu=[-Node1_Inpu -Node2_Inpu -Home_Node_Inpu];

    %create YLnpu - a matrix of the line admittances
    ZLnpu=RL1pu+j*n*XL1pu;
    YLnpu = zeros(M,M);
    for a=1:1:M
        for b=1:1:M
            if ZLnpu(a,b) ~= 0,
               YLnpu(a,b) = 1/ZLnpu(a,b);
            end
        end
    end



YLnpu=YLnpu+YLnpu.';
Ynpu = -YLnpu;

%Diagonal values are initialized to self admittances.
for a=1:1:M
    Ynpu(a,a)=Node_Ynpu(a);
end

%Node self admittance is added to the sum of the line admittances
%for that node.
for a=1:1:M
    for b=1:1:M
        if a ~= b, Ynpu(a,a) = Ynpu(a,a)+ YLnpu(a,b);
        end
    end
end

Znpu=inv(Ynpu);
Node_Vnpu=abs(Znpu*(Node_Inpu).').';
Node_Vn=Node_Vnpu*Vb_base;

Node_Vpu=[Node_Vpu; Node_Vnpu];
Node_V=[Node_V; Node_Vn];
 end

%Calculate Node Voltage THD and RMS
 Node_V_dist(M)=0;
 Node_V_RMS(M)=0;
for a=1:1:M
    for n=1:1:6
        if n~=1
            Node_V_dist(a)=Node_V(n,a)^2+Node_V_dist(a);
        end
        Node_V_RMS(a)=Node_V(n,a)^2+Node_V_RMS(a);
    end
    Node_V_dist(a)=sqrt(Node_V_dist(a))/Node_V(1,a)*100;
    Node_V_RMS(a)=sqrt(Node_V_RMS(a));
```

```
end

fprintf('NODE RMS VOLTAGES [V]\n')
for a=1:1:M
fprintf('V%d = %6.1f \n',a,Node_V_RMS(a))
end

fprintf('\nTOTAL HARMONIC DISTORTION\n')
for a=1:1:M
fprintf('Node %d THD = %3.2f %%\n',a,Node_V_dist(a));
end
fprintf('\nCRMS VOLTAGE HARMONICS [V]\n')
for a=2:1:N/2+1
fprintf('n = %d: \n',2*a-1);
    for b=1:1:M
        fprintf('V%d  =%6.1f,  ',b,Node_V(a,b))
    end
fprintf('\n\n')
end
```

VITA

Paul Haley was born in Anchorage, Alaska in 1987. In 1994 his family relocated to Kenner, Louisiana which is where he spent most of his childhood. He graduated in 2006 from Grace King High School in Metairie, where he developed an appreciation for science and mathematics. Paul attended Louisiana State University where he received the Bachelor of Science degree in Electrical Engineering in 2010. Through his experiences tutoring other students he discovered that he enjoyed teaching, and he returned to Louisiana State University for graduate school with the goal of attaining an academic career. He is currently pursuing a doctoral degree in Electrical Engineering.